Journal of Human Evolution 59 (2010) 234–255

Contents lists available at ScienceDirect

Journal of Human Evolution

journal homepage: www.elsevier.com/locate/jhevol

The stratigraphy of the Middle Stone Age sediments at Pinnacle Point Cave 13B (Mossel Bay, Western Cape Province, South Africa)☆

Curtis W. Marean [a,*], Miryam Bar-Matthews [b], Erich Fisher [c], Paul Goldberg [d], Andy Herries [e], Panagiotis Karkanas [f], Peter J. Nilssen [g], Erin Thompson [h]

[a] Institute of Human Origins, School of Human Evolution and Social Change, PO Box 872402, Arizona State University, Tempe, AZ 85287-2402, USA
[b] Geological Survey of Israel, 30 Malchei Israel Street, Jerusalem 95501, Israel
[c] Department of Anthropology, University of Florida, Gainesville, FL 32611, USA
[d] Department of Archaeology, Boston University, 675 Commonwealth Ave., Boston, MA 02215, USA
[e] School of Medical Sciences, Faculty of Medicine, The University of New South Wales, Sydney NSW 2052, Australia
[f] Ephoreia of Palaeoanthropology-Speleology, Ministry of Culture, Greece
[g] CHARM, PO Box 176, Great Brak River, 6525 Mossel Bay, South Africa
[h] School of Human Evolution and Social Change, PO Box 872402, Arizona State University, Tempe, AZ 85287-2402, USA

ARTICLE INFO

Article history:
Received 14 July 2008
Accepted 21 May 2010

Keyword:
Origins of modern humans

ABSTRACT

Pinnacle Point Cave 13B (PP13B) has provided the earliest archaeological evidence for the exploitation of marine shellfish, along with very early evidence for use and modification of pigments and the production of bladelets, all dated to approximately 164 ka (Marean et al., 2007). This makes PP13B a key site in studies of the origins of modern humans, one of a handful of sites in Africa dating to Marine Isotope Stage 6 (MIS 6), and the only site on the coast of South Africa with human occupation confidently dated to MIS 6. Along with this MIS 6 occupation there are rich archaeological sediments dated to MIS 5, and together these sediments are differentially preserved in three different areas of the cave. The sediments represent a complex palimpsest of geogenic, biogenic, and anthropogenic input and alteration that are described and interpreted through the use of a variety of macrostratigraphic, micromorphologic, and geochemical techniques. Three independent dating techniques allow us to constrain the age range of these sediments and together provide the stratigraphic context for the analyses of the material that follow in this special issue.

Introduction

The stratigraphy of an archaeological site forms the contextual foundation for all other interpretations drawn from the excavations of that site. Caves are natural attractors for people and other animals (Brain, 1981), who then regularly deposit the remains of their activities. Caves are also natural sediment traps, which due to their enclosed form then act as good but not perfect protection from erosive forces (Goldberg and Sherwood, 2006). This fact often results in accumulations of long depositional sequences that traditionally have been the focus for reconstructing through proxy means the character of ancient climates, environments, and animal and human behavior (Laville et al., 1980; Woodward and Goldberg, 2001). Archaeologists working in the stone age continue to rely on cave sequences to develop foundations for regional sequences of change in the archaeological record (Clark, 1959; Sampson, 1971; Deacon and Deacon, 1999; Marean and Assefa, 2005).

However, caves pose complex depositional environments where mechanical and chemical processes transform the deposits through geogenic, biogenic, and anthropogenic activity, complicating interpretations of context and geochronology (Weiner et al., 1993; Karkanas et al., 2000). Accurate interpretation of this depositional environment rests on careful field technique of observation and recording, field and laboratory methods for disentangling the processes, and cross-disciplinary integration of all the sources. Importantly, clear explication of the observations and interpretations of this sedimentary system is essential for scientists intent on analyzing the materials and critically evaluating the reasoning behind contextual and geochronological inferences.

Pinnacle Point Cave 13B (PP13B) is a cave with a complex history of deposition, erosion, and alteration. The research team working there has employed a wide range of techniques to reconstruct and understand this sequence and has grounded these techniques in

☆ This article is part of 'The Middle Stone Age at Pinnacle Point Site 13B, a Coastal Cave near Mossel Bay (Western Cape Province, South Africa)' Special Issue.

* Corresponding author.
E-mail address: curtis.marean@asu.edu (C.W. Marean).

0047-2484/$ – see front matter © 2010 Elsevier Ltd. All rights reserved.
doi:10.1016/j.jhevol.2010.07.007

state of the art field recording methods based on total station measurements of all observations. Micromorphology, geochemistry, and archaeomagnetics joined to macrostratigraphic field and laboratory techniques have allowed us to develop a robust understanding of this sequence. This provides an excellent contextual foundation for the analyses that follow in this volume, and eventually in later analyses and reports. In this paper we describe the nature and age of the major stratigraphic units in PP13B, drawing on a wide set of observations, but with the emphasis on macrostratigraphic field and laboratory observations and analyses.

Geological background

Pinnacle Point (PP) is the area surrounding a small headland in a cliffed coast on the Indian Ocean on the central south coast of South Africa, approximately 10 km west of the Mossel Bay point (Fig. 1). Pinnacle Point is a formal geographic location and is now the location of a large golf and resort development above the cliffs. We recognize it as a locality around which are concentrated a wide variety of archaeological, paleontological, and geological localities of paleoanthropological interest. Our research has focused on a 2 km stretch that falls mostly to the east of the Pinnacle Point headland.

From Pinnacle Point to the Mossel Bay point, the heavily dissected coastal cliff displays caves, gorges, arches, and stacks that signal cliff dissection and retreat, a process enhanced by repeated high sea levels (Bird, 2000). This ongoing cliff retreat provides debris for the formation of rocky intertidal zones nearby the caves. The prevailing wind and swell are from the southwest (Tinley, 1985), which in concert with structural factors has created a classic "log-spiral" or "headland-bay" coast (Dardis and Grindley, 1988), with beaches often formed in the half moon bays on the protected side of the headlands. This is the case just several hundred meters west of PP13B. Further to the east, the Mossel Bay point and bay form a mature and well-developed half moon bay with an extensive beach. The result is the presence of two distinctive intertidal systems, sandy and rocky, that afford differing shellfish collecting opportunities (Fig. 2).

The coastal cliffs are highly folded and faulted exposures of the Skurweberg Formation of the Paleozoic Table Mountain Sandstone (TMS) Group, comprising coarse grained, light-gray quartzitic sandstone, with beds of varying thickness and consolidation, often covered with lichens (Fig. 3). The dip varies strongly along the coast, ranging from 10 to 75° (South African Geological Series 3422AA, 1993). Shear zones with boudinage features cut through the TMS (Fig. 3a and b), fault breccias of varying thickness fill these zones, and the caves and rockshelters are found in these eroded fault breccias (Fig. 3a and b). Unlithified dunes, aeolianites, calcarenites, and calcretes cap the TMS throughout the area and are mostly referable to the shallow marine Quaternary Klein Brak, and

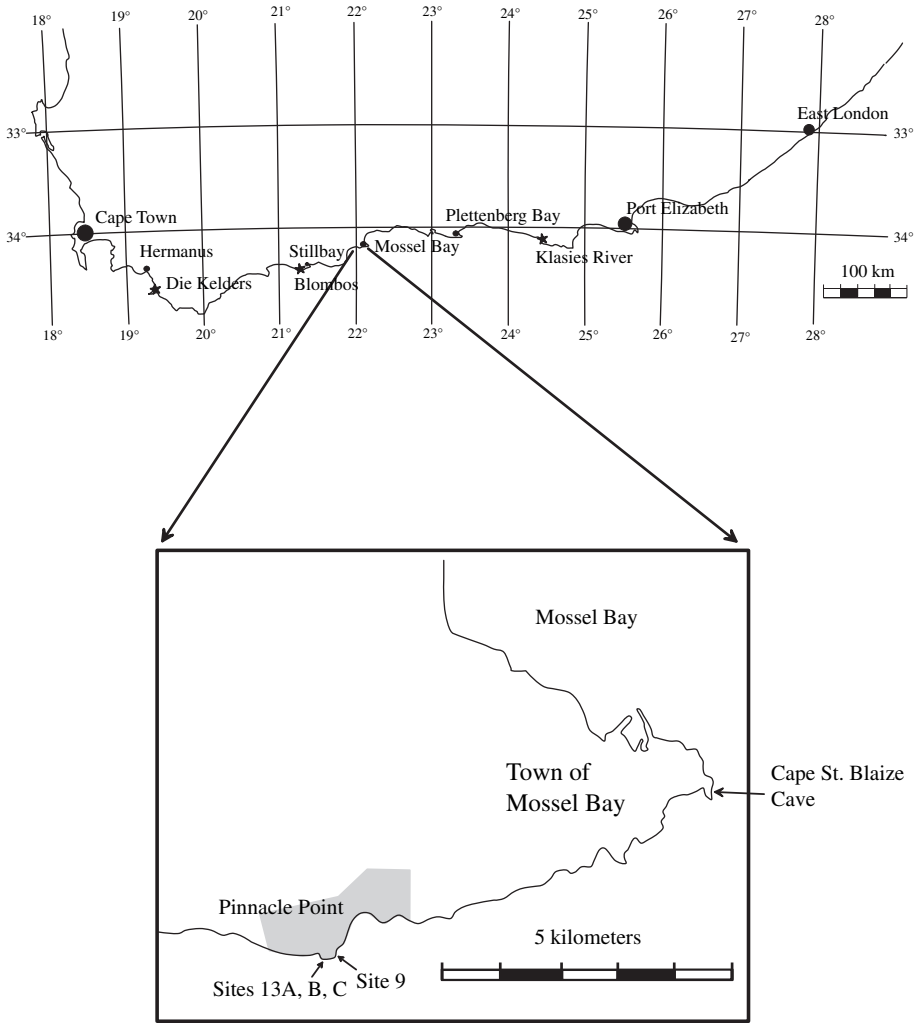

Fig. 1. Map of southern Africa showing the location of Mossel Bay (above) and a detail showing the position of Pinnacle Point relative to Mossel Bay.

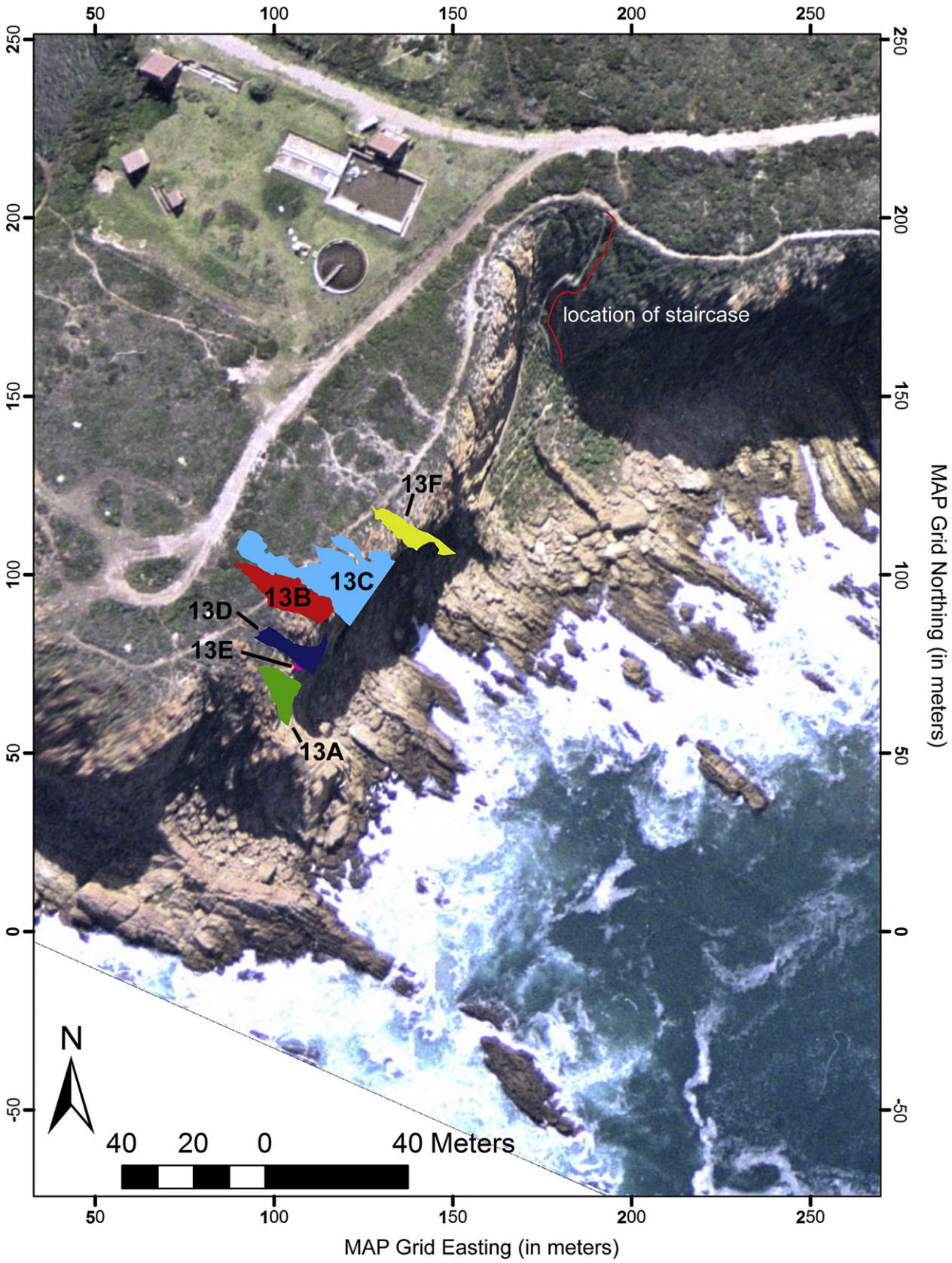

Fig. 2. An aerial photograph of the Site 13 Complex area prior to development showing PP13B and other sites mentioned in the text in the cliff face. The aerial photograph is rectified to the MAP grid.

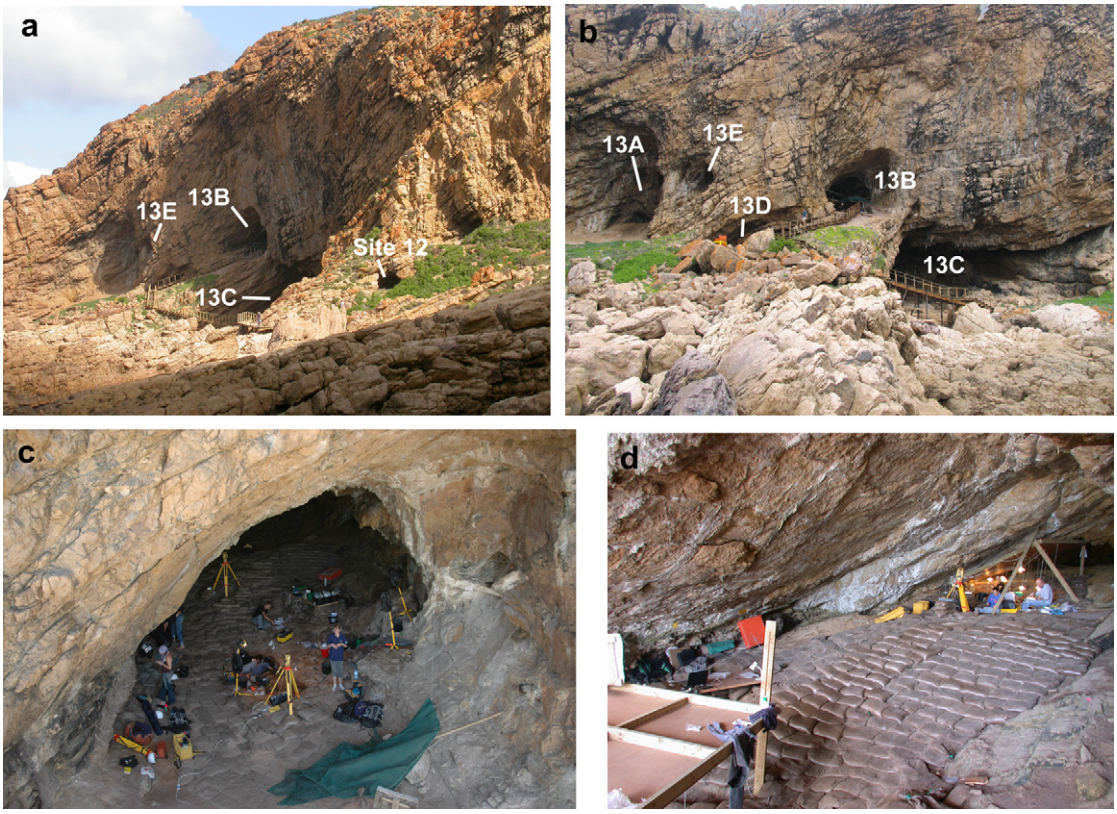

Fig. 3. Various views of the Site 13 Complex and PP13B. (a) View of the cliff from the northeast looking at the Site 13 Complex indicating several of the caves, (b) view of the cliff from the southeast looking at the Site 13 Complex indicating several of the caves, (c) PP13B mouth of the cave with photographer hanging from rope, and (d) PP13B showing western excavations in back and roof of eastern excavations in front.

aeolian deposits of the Waenhuiskrans and Strandveld Formations (Malan, 1987, 1991; Viljoen and Malan, 1993). These are found in extant caves (Fig. 3c), in the remnants of collapsed caves, cemented to the cliff walls, and on the landscape. Sonar studies have shown that these dune systems are partially preserved on the submerged continental shelf and likely connected to the better-preserved terrestrial systems at Sedgefield and Wilderness (Birch et al., 1978; Flemming, 1983; Flemming et al., 1983). Their relevance derives from the fact that at times they sealed the caves from occupation (Marean et al., 2007) and can be an informative source of paleoenvironmental information.

The edge of the continental shelf is approximately 120 km offshore in this area and the coastal platform declines in elevation gradually from the current coast to the shelf edge (Van Andel, 1989), so that extensive coastal landscapes formed where populations may have resided during sea level regressions (Fisher et al., 2010). The offshore platform was the source for much of the aeolian sands that comprise the extensive ancient dune systems on land (Illenberger, 1996), under sea (Dingle and Rogers, 1972; Flemming et al., 1983), and in the caves (Birch et al., 1978).

A large number of coastal caves and rockshelters (>20) occur in the nearly vertical coastal cliffs in the thicker shear zones where substantial fault breccias had formed and the caves typically coincide with less steeply dipping beds (10–40°). The primary mechanisms for cave development include the formation of the shear zones, followed by movement along these shear zones and erosion at the contact, cementation of the breccia, mechanical erosion by high sea levels, and in some cases collapse. The caves cluster at two heights: +3–7 m asl (meters above sea level) and +12–15 m asl. Since the coast has been tectonically stable through the Quaternary (Partridge and Maud, 1987; Partridge, 1997) these likely represent separate high sea levels, and we are currently seeking to ascertain these times of cave formation.

While TMS is acidic and acidizes groundwater flowing through it, the water entering the caves has been buffered by the calcium carbonate rich formations capping the TMS, as at Klasies River (Singer and Wymer, 1982). Abundant calcite formations are present in the caves and rockshelters, particularly along joints and bedding planes (Fig. 3c). Small (1–10 cm) to large (>1 m) stalactites and stalagmites are present in many of the caves, and flowstone formations are present in all the caves, often intercalated with archaeological deposits and almost always occurring behind aeolianite remnants. Various phases of speleothem formation can be identified that mark periods of cave entrance enlargement and reduction. The intercalation of speleothem with sediments affords the opportunity to conduct both uranium–thorium dating (U–Th) and optically stimulated luminescence (OSL) on intercalated sediments.

At the tip of PP are a series of caves/rockshelters (PP13A-G) within a stretch of 200 m of cliff space; these are grouped as the site PP13 cave complex (Fig. 3). Our work shows they shared formational and depositional histories and probably at one time some of them shared intercalated sediments (Marean et al., 2004, 2007). We have mapped most of the caves and developed 3D models of these integrated into our 'paleoscape' model (see Marean et al., 2007: their Supplementary Video; Fisher et al., 2010). Several of these caves are of particular interest here. Strangely, we have not yet identified LSA occupation at any of the PP13 sites, but MSA deposits are common.

We tested excavated PP13A in 2000 (Marean et al., 2004). This now collapsed cave has an unlithified dune in its mouth with well-preserved MSA deposits near to the surface. PP13C, a large cave that

undercuts PP13B (Fig. 3) and whose mouth is within the high tide zone, has an MSA deposit in the back, as well as a dense lag deposit of MSA lithic artifacts in the front. Flowstones cover the TMS in the back of the cave, stalactites hang from the roof, and cemented sands are present along the walls and ceiling. PP13D is a cave whose sediments currently lie between +8 and 10 m. Speleothems are present in the cave, and the distribution of aeolianite shows it was once sealed. PP13E is a small cave that retains a Lightly Cemented MSA deposit (LC-MSA; described below) extending from the walls between +15 and 18 m. PP13F is an inverted V-shaped cave with sediments that lie between +6 and 8.5 m. Cemented sands and red coralline algae formations are cemented to the walls and in several locations flowstones drip over the eroded surfaces of these formations. PP13G is a small cave with no archaeological deposit at +14.5 m. It has a shelly beach with a thick clean speleothem stratified above.

PP13B is shown in Figure 4 in profile and in plan view. To produce this profile we measured with the total station approximately 800 points individually coded to the cave rock and all the geological features. From this a 3D TIN of the cave and all geological features was produced and integrated into our overall paleoscape model, a 3D offshore–onshore digital model of coastline change over the last 420 ka (Fisher et al., 2010). Then, using a program designed by E.F., we sliced the cave, cliff, and coastal platform to produce the profile. The profile base is the sediment surface and not the rock floor.

PP13B has a circular mouth that faces east and overlooks the ocean. From the back of the cave the mouth resembles a ship's

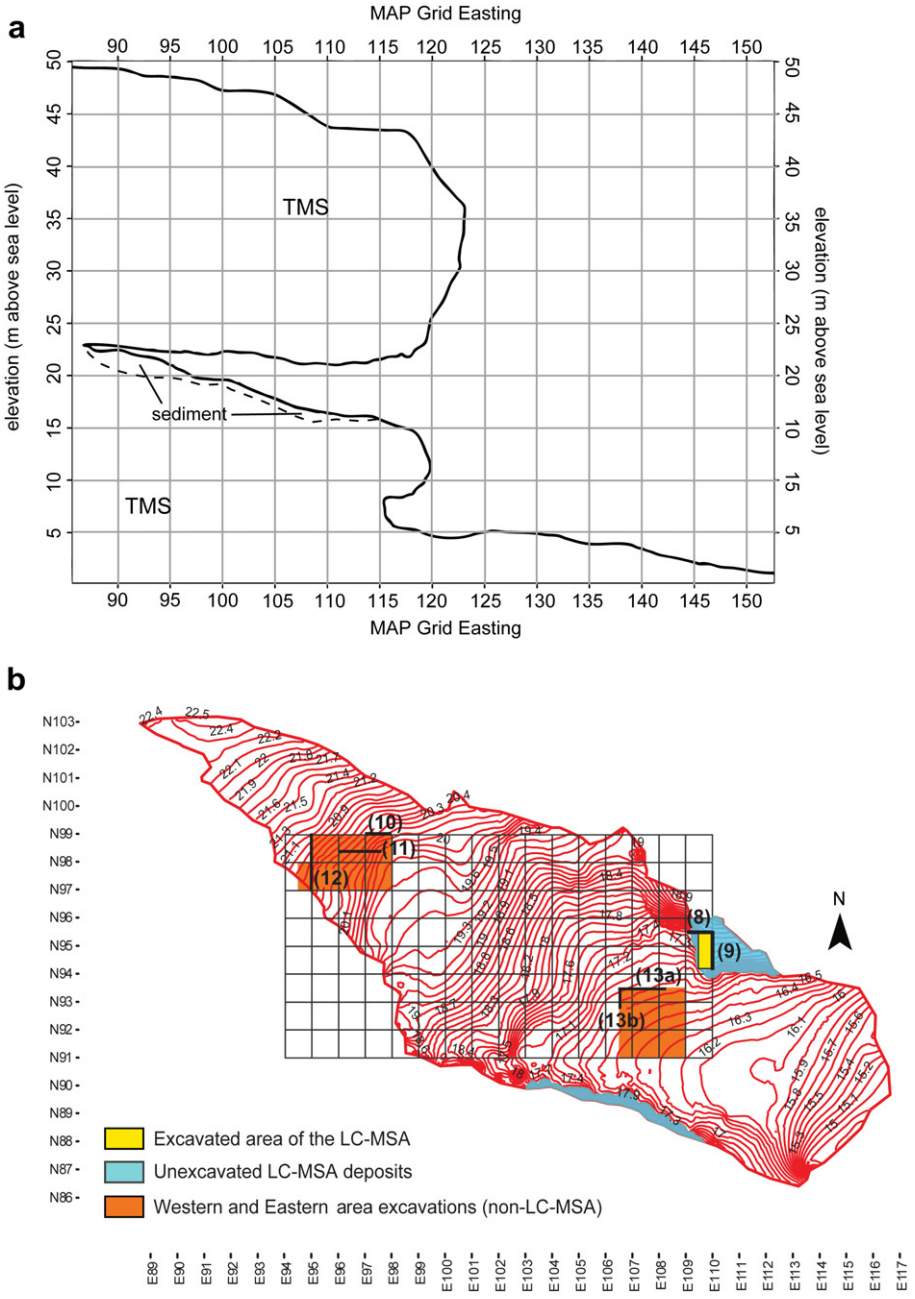

Fig. 4. (a) Profile of PP13B as produced from slicing the 3D model in MAP grid, and (b) plan of PP13B in MAP grid.

porthole looking out to sea. The mouth measures about +15 m and the roof at the mouth is about 7 m above the floor, narrowing as the sediments slope up toward the back. There is sufficient room to allow a person to walk or crawl except for the few meters at the very back. The dimensions of the cave are roughly 30 m long by 8 m wide, and it is oriented with its long axis in a roughly East/West direction. One can experience the cave in 3D with the Supplementary Video published elsewhere (Marean et al., 2007).

Several layers of TMS of varying erosional resistance form the cave walls and ceiling. Friable fault breccia that once filled the cave is now mostly eroded away except for at the very back of the cave. Speleothem is present on the roof and walls at various locations, as are remnant cemented sands. Archaeological sediments are visible as three distinct sets: a remnant on the north wall, a remnant on the south wall, and surface sediments that stretch from the front to the back of the cave. Near the front the surface sediments are nearly horizontal and then they begin sloping up more steeply toward the back (Fig. 4). Nearer the front the surface sediments are composed of wind blown sand, silt, and ash from fires, and then toward the back they become more yellow and coarse grained, being composed of fault breccia material that has spalled off the ceiling rather recently. MSA sediments are stratified directly below these surface sediments. We excavated into the surface sediments in two areas (Fig. 4): near the front (Eastern area) and near the back (Western area).

On the north wall of the cave near the mouth is a wedge of sediment with a naturally eroded profile that exposes archaeological and geological layers (Figs. 3c and 4b). Near to the cave opening is a thick calcareous formation that sits atop this wedge of sediment, in one area extending to the roof and into a crack as a pillar, and behind this is a clean speleothem (flowstone) capping the deposit. The remnant of a dune that once sealed the cave is clearly visible on the cave wall, connecting to the upper dune overlying the archaeological deposits. All are cut by an erosion event that leaves a profile that resembles an excavated profile, but is the result of natural forces. We conducted excavations into this area (Marean et al., 2007) and it is called the Northeastern area and has only LC-MSA deposits.

On the south wall of the cave is a second set of LC-MSA sediments (Fig. 4b). They stretch from near the mouth of the cave to about the middle of the cave where they meet the surface sediments and likely plunge under those sediments. We have not resolved the nature of the contact between these two sets of sediments. The southern LC-MSA sediments resemble the northern LC-MSA sediments, but there are some distinctions. The southern sediments have larger and more frequent roof spall, larger stone tools, and larger shellfish. Also, the horizontal exposure is far less, though given the bedding plane of the cave TMS (which slopes to the south) it is likely that there is substantial LC-MSA preserved as a wedge in that unexposed area. We did not excavate into the southern LC-MSA sediments, although we have taken a complete micromorphology sample, photographed the section, and dated the section with OSL.

The area within PP13B is well protected from the elements and is pleasant even during the most unpleasant of storms. During the mornings, the sun shines on the front 25% of the floor for several hours and then disappears behind the cliffs. Overall, the cave provides a well-sheltered environment that is still attractive to fishermen, who generally place their fires at the mouth of the cave.

Field methods

Our field methods are described elsewhere (Marean et al., 2004; Dibble et al., 2007), so here we highlight the critical aspects. We employ an arbitrary three-dimensional coordinate system (grid) called the MAP grid. Once established, we corrected the *z* for true orthometric height as defined by the South African National Coordinate (SANC) reference system. Our analysis of approximately 40 years of hourly measurements from the Mossel Bay and Knysna tide gauges shows that current mean sea level is about 1 m above orthometric zero and rising. Since orthometric zero is traditionally equated with mean sea level, we will refer to zero elevation as sea level, with the proviso that rising sea level has negated this relationship. More recently we have tied our MAP grid to the updated SANC that employs the World Geodetic System 1984 (WGS84) as their base and the new Hartebeesthoek94 Datum. The MAP grid can be converted to this system with a two-dimensional conformal coordinate transformation (Wolf and Ghilani, 2002), and from there to latitude and longitude following the Gauss Conform Projection used by South Africa. Since this conversion occurred midway through the excavations at PP13B, our presentation of the PP13B material will occur in the MAP grid, while all future sites have already shifted to SANC.

The MAP coordinate system is oriented to magnetic north and grid coordinates advance positively to the north (*x*-axis) and east (*y*-axis). A 1 m square is named by the planar coordinates of its southwest corner. We excavated within 50 cm quadrants within squares, and these are named by their bearing: NE, NW, SE, and SW. Excavations were conducted within these quadrants following natural stratigraphic units (layers, features, etc.), and thus all finds have at least an assignment to square, quadrant, and stratigraphic unit, while most finds have a precise 3D coordinate as well. Sediment volumes were measured during excavation and bulk samples of sediment were taken from every unique stratigraphic unit. All finds that were seen by the excavator were plotted (henceforth called plotted finds) in *x*-*y*-*z* coordinates by total station directly to a handheld computer outfitted with a barcode scanner to record specimen numbers and provenience information (Dibble et al., 2007).

All recording was done to forms (supplemented by notebooks), and those were typed into a form-based database system. All features and stratigraphic units were drawn to graph paper and their shape and topography were shot in directly by total station to handheld computer. All measurements on site are made with total stations due to the inherent error involved in tape measure use, including everything from plotted finds to section drawings. All non-plotted materials were gently wet sieved with fresh water through a nested 10-3-1.5 mm sieve. These were dried, packed in plastic bags, and transported to the field laboratory where they were sorted into major analytical categories (lithic artifacts, fossil bones, etc.) and some preliminary analyses were performed. All plotted finds were labeled with their specimen number in black India ink. Materials were then sorted into analytical groups and provided to specialists for analysis.

General procedures for stratigraphic analysis and presentation

The excavations at PP13B were conducted within small stratigraphic lenses and features, collectively titled stratigraphic units (StratUnits). The volume of these is typically less than one bucket of sediment and as such is far too small for meaningful statistical analysis of their contents. These StratUnits were then grouped into larger stratigraphic aggregates (what many archaeologists may call layers, or facies; Reading, 1996) based on more general geogenic and anthropogenic characteristics. Each stratigraphic aggregate reflects a homogeneous set of formation processes recognized by field and micromorphological observations. For example, this could be a sandy layer between two charcoal layers or a continuous charcoal lens.

This grouping was done in a series of steps. First, StratUnits were assigned to informal stratigraphic aggregates in the field during their excavation or immediately thereafter. This was done by the directors in consultation with the excavators and was based primarily on macroscopic criteria. Then, total station shots of StratUnits were projected onto rectified section drawings and photographs in vertical perspective to check the consistency of the assignments with the recorded section information. Three-dimensional point clouds were also generated, with individual stratigraphic aggregates color coded to again check for consistency. Finally, all plotted finds were attached to their stratigraphic aggregate, and these were then projected onto the section drawings and photographs to do another check of the internal consistency. Micromorphological observations and interpretations of formation processes were then joined to develop overall facies level reconstructions of the sequence of deposition, alteration, and erosion. The stratigraphic aggregates and facies are described below. For each stratigraphic aggregate, we note whether it was once called by a different name, either in publication or prior reports. Dating is accomplished with a combination of U–Th, OSL, and checking against the output of the paleoscape model (see below).

U–Th dating (also known as uranium series, U-series, ^{230}Th/U) when conducted on speleothem with low amounts of detritus offers the most accurate and precise dating method within the last 500 ka. With U–Th dating, speleothem can be dated in calendar years with a precision nearing $\pm$0.5% at 2σ. The technique does not require any age calibration or reservoir correction (McDermott, 2004) and is underutilized in paleoanthropology. U–Th at PP13B was conducted only on speleothem with low amounts of detritus, and all specimens have been studied petrographically for analysis of crystal structure. Speleothem at PP13B was found in two relationships with sediments. In some cases speleothem was found intercalated with sediments, flowing or dripping directly onto a surface. The nature of this contact was in all cases verified with micromorphology, a step we consider essential to the accurate use of speleothem dating in archaeology. Given the high precision and accuracy of U–Th on clean speleothem, these ages provide excellent minimum ages of everything stratified below. Second, speleothem pieces were found stratified within sediments, having detached from their growth position and fallen into the sediment. We carefully searched for these during excavation and after excavation in the sieves. Since these pieces stopped growing at least at the time of detachment, they provide a maximum age for the position of the speleothem and all sediments above. The precise U–Th estimates in some cases allow us to shorten the error ranges associated with some OSL age estimates, as discussed further below. The U–Th ages and methods are in the Supplementary Online Material (SOM) that appears with the online version of this article (doi:10.1016/j.jhevol.2010.07.007).

OSL provides an age estimate of the last time the sediment was exposed to radiation (sunlight or heat) sufficient to bleach the grains being dated (Murray and Wintle, 2000), and we provide here two different types of OSL age estimates. Most of the age estimates use the standard SAR protocol applied to single grain dating (see Jacobs [2010] for details). The maximum age that conventional SAR protocol methods can produce is a function of dose rate. At Pinnacle Point, so far conventional SAR OSL appears to begin to saturate at about 200 ka. Therefore, Jacobs (2010) has turned to and refined a new approach (TT-OSL) that allows far older age ranges to be attained. We use it here for the first time in an archaeological site. Most OSL ages come from locations where we also conducted micromorphology. Micromorphology significantly enhances our ability to understand sedimentary processes potentially problematic for OSL.

Finally, our age estimates benefit from the production of a 3D GIS (Marean et al., 2007; Fisher et al., 2010) of the landscape and seascape that we call the paleoscape model. Sea level has fluctuated dramatically over the span of occupation and what we see today outside the cave mouth bears little resemblance to most moments in Pleistocene time. However, bathymetric data joined to sea level curves facilitates the development of a model that allows us to project the coastline position during slices of time in the past (Fisher et al., 2010). Since regular transport of shellfish rarely occurs beyond 10 km (Erlandson, 2001), in those layers where shellfish are present we can check age estimates by calculating distance to the coast to see if it is within this distance.

In the summary presented here, all techniques are used to develop an overall site chronology, and our primary goal is to provide a conservative estimate of the age range of the stratigraphic aggregates. We follow the terminological recommendations by Colman et al. (1987): 1) the radiometric (OSL), isotopic (U–Th), and geomorphic (sea-level model) techniques used here do not produce dates (which are specific points in time on a calendar), but rather ages that should be expressed as a range; and 2) we treat the ages as age range estimates, in our case bracketed by 1σ. OSL age estimates often have significant errors that, at times, are sufficient to frustrate precise assignment of a stratigraphic aggregate to a narrow range of time. In some cases we have a U–Th age stratified within or above and we use the precision of that technique to constrain the age range (Fig. 5).

Table 1 provides a conservative range of time represented by each stratigraphic aggregate. Some aggregates lack any radiometric or isotopic age estimates, and these are indicated by being in italics. However, we provide age estimates based on context, since their minimum age can be no less than the minimum age for overlying stratigraphic units, and their maximum age can be no more than the maximum age for underlying stratigraphic units. We also assume that the U–Th age on the flowstone of 91.6 $\pm$ 0.5 ka marks the closing of the cave at least by 91.1 ka, that the youngest U–Th age and the ^{14}C age indicate that the cave opened at least by 38.9 ka, and that no anthropogenic input can date between 91.1 and 38.9 ka, or approximately 91–39 ka.

In the discussion below, it is implied that we are citing the following papers for each of these materials: OSL (Jacobs, 2010), magnetic susceptibility (Herries and Fisher, 2010), micromorphology (Karkanas and Goldberg, 2010), and orientation and inclination studies of the plotted finds (Bernatchez, 2010). Figure 6 provides an overall summary of the age ranges and stratigraphic relations of the stratigraphic aggregates. Figure 7 and Table 2 provide for each stratigraphic aggregate the number of lithic artifacts per m^3, the sum weight (g) of lithic artifacts per m^3, and the mean magnetic susceptibility as proxies of the intensity of discard of lithic artifacts and burning. Marean (2010) provides further density data. The densities of materials fall into three basic groups that largely follow the lithic artifact densities. In the text below, we use the following classes to describe density: low (lower third), moderate (middle third), and high (upper third).

Northeastern area

The Northeastern LC-MSA sediments occur cemented to the northern and southern walls (Fig. 4b). We review and expand earlier descriptions (Marean et al., 2007). We concentrated our efforts on the northern deposits as these are more horizontally exposed. The northern LC-MSA deposits occur as a perched wedge of sediment with two main exposed sections. One runs roughly north to south on the western side of the sediment wedge and then turns and runs roughly east to west on the southern side. Due to the small amount of preserved sediment, and our initial impression that this material would date to MIS 6 (and thus be quite rare), we conducted a limited excavation to preserve sediments for future

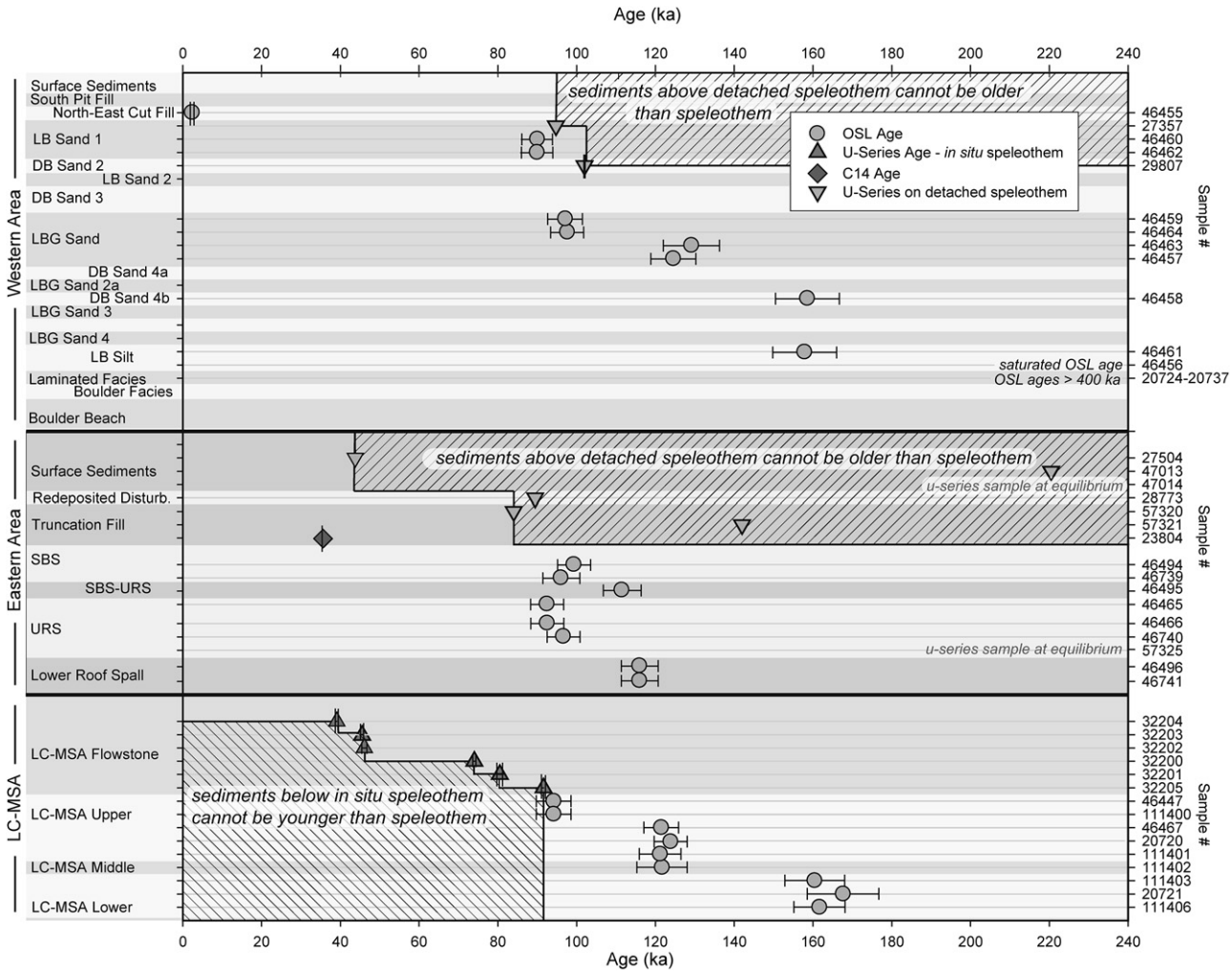

Fig. 5. The radiometric and isotopic ages produced to date for PP13B with 1σ plotted as an error bar. The sample numbers are listed on the right axis, the stratigraphic aggregates to the left, and the stratigraphic aggregates are arranged by excavation area. The figure also shows when the cave was closed by a dune, as determined by *in situ* flowstone formation in the LC-MSA, and minimum age constraints as indicated by detached speleothems in the sediments.

investigators. These sections reveal varying densities of archaeological finds and burnt organic materials concentrated in clear lenses that are roughly horizontal to the cave floor bedding plane. We excavated into these exposed sections (Figs. 8 and 9).

The initial LC-MSA excavations in 2000 involved a small test excavation of one roughly 50 cm by 50 cm quad into the exposed and eroded section and are reported in Marean et al. (2004). We extended the excavations into the LC-MSA in the 2005 October–November and 2006 May–June field seasons by excavating two more quads to the north of the quad excavated in 2000. The excavation into the LC-MSA was complicated by the cement like calcareous horizon capping the archaeological horizons and the semi-cemented nature of the deposit. We used an angle grinder to cut through this capping, lifted it off, and it separated reasonably cleanly from the underlying archaeological sediment. The LC-MSA Upper is heavily cemented and much of it was removed as blocks. The LC-MSA Middle and Lower were less cemented and the sediments could be excavated quite easily and finds plotted.

In Marean et al. (2004), we grouped the main part of the section into a single stratigraphic aggregate because the sample size of lithic artifacts was quite small and the short section provided little firm stratigraphic evidence. A micromorphology sample (20249) was taken from the entirety of this section in 2003 and has been studied. Like the other excavated areas, micromorphological observations fail to identify any significant turbation from burrowing insects or mammals. The 2005 and 2006 excavations provided a thicker section from a wider extent, and that, coupled with some new stratigraphic observations, have allowed us to the refine our divisions of the stratigraphy. We now recognize the following stratigraphic sequence.

Bedrock The Bedrock is a TMS at the base of the sediments and is visible in both Figures 8 and 9. Much of it is rounded by water action, and this water action is probably associated with the beach encountered at the base of the excavations in other excavation areas. We think this is associated with high sea levels, and the ages reported refer to the likely age of the last high sea level event that washed into the cave.

LC-MSA Lower The LC-MSA Lower is the lowest set of sediments of the section and is the archaeologically richest of all the LC-MSA sediments. This is the least cemented of all the layers in the LC-MSA. There are multiple lenses of carbonaceous material that appear heavily burnt. The presence of anthropogenically fire altered material (Herries and Fisher, 2010) has been documented by frequency dependent magnetic susceptibility (MS). The mean MS is high relative to other layers (Fig. 7), consistent with the identification of regular burning, and lithic artifact densities are

Table 1
Adjusted age ranges for all stratigraphic aggregates at PP13B ordered oldest at bottom to youngest at top[a]

Stratigraphic aggregate	Area	Adjusted minimum	Adjusted maximum
Surface sediments	Western	*0*	*0*
Surface sediments	Eastern	*0*	*0*
Re-Deposited Disturbance	Eastern	*0*	*0*
Northeast Cut Fill	Western	2	3
South Pit Fill	Western	*0*	*39*
Truncation Fill	Eastern	35	*39*
LC-MSA Upper Flowstone	Northeastern	39	*92*
LC-MSA Upper (Upper Dune)	Northeastern	91	98
LB Sand 1	Western	91	94
DB Sand 2	Western	91	102
LB Sand 2	Western	*91*	*102*
DB Sand 3	Western	91	102
Shelly Brown Sand/Upper Roof Spall	Eastern	91	98
Lower Roof Spall	Eastern	106	114
LBG Sand	Western	94	134
LC-MSA Upper (Lower Dune)	Northeastern	115	133
LC-MSA Middle	Northeastern	120	130
DB Sand 4a	Western	*117*	*166*
LBG Sand 2	Western	*117*	*166*
DB Sand 4b	Western	152	166
LBG Sand 3	Western	*152*	*349*
DB Sand 4c	Western	*152*	*349*
LBG Sand 4	Western	*152*	*349*
LC-MSA Lower	Northeastern	153	174
LB-Silt	Western	*152*	*349*
Laminated Facies	Western	349	414
Boulder Facies	Western	349	*Unknown*
Bedrock	All areas	349	*Unknown*

[a] Age ranges in italics do not have radiometric ages but rather represent estimates based on context.

high. Micromorphology shows that some of these are *in situ* combustion features and some appear trampled. These are very fine *in situ* fires, with some hearth cleanout separating them.

Micromorphology also shows that there is less ash in the LC-MSA Lower than in the LC-MSA Middle. The density of lithic artifacts and faunal remains is high throughout the LC-MSA Lower, both in these burnt lenses and between them as well. Marine shell density is moderate, but varies horizontally: it is rare to the south and increases to the north (Marean et al., 2007). Micromorphology shows that this is not the result of dissolution of shell to the south, suggesting that shell was preferentially deposited against the cave wall, either through direct discard or secondarily through site maintenance.

There is a slight slope to the plotted finds, with most between 0° and 15°; however, a substantial portion slopes between 15° and 30°, but with little or no dramatic or random changes to slope that would indicate intrusions or disturbances. The layers slope gently down from north to south and where there is bedrock at the base of the sequence the layers dip and rise in concert with the rock surfaces. The distribution of plotted finds follows this grade.

There is an observable change in the section, and also in the ash content and level of cementation, between the Lower and Middle LC-MSA. The contact between the Lower and Middle LC-MSA is abrupt in some areas. It appears likely that the contact represents slight erosion, lack of deposition with exposure, or trampling of the top of the LC-MSA Lower. This is consistent with the significant difference in age between the LC-MSA Lower and Middle (~30 ka). However, the micromorphology does not suggest a major change in sedimentation.

The three LC-MSA Lower OSL ages result in a weighted mean age of 162 ± 5 ka. This age is concordant with a short and rare event in MIS 6 when the sea level rose and brought the coast within 5 km of the cave, which is consistent with the presence of shellfish in the sediments (Marean et al., 2007; Fisher et al., 2010). The adjusted maximum and minimum ages are 174 and 153 ka, respectively.

LC-MSA Middle The LC-MSA Middle includes multiple lenses of dark organic material that micromorphology shows have charcoal and *in situ* hearths. The mean MS and lithic artifact densities are moderate (Fig. 7). Much of the deposit is ash. Micromorphology shows that there is evidence for trampling. Cobbles and roof fall are common. Marine shellfish densities are high and it shows the same horizontal pattern as with the LC-MSA Lower, where shell density increases to the north.

One of the main diagnostic features of the LC-MSA Middle is the presence of white pipes that penetrate into it and can be seen in cross-section in our section photographs (Figs. 8 and 9). Micromorphology shows that these are the remnants of ancient roots that penetrated into this layer, disturbed the layer, and then were subsequently replaced with calcite. The slope line of the plotted finds shows that, while there is a general tendency for the finds to be parallel to the slope of the sediments, there are multiple examples of finds dipping abruptly down, suggesting some downward disturbance, perhaps related to root penetration. The overall slope of finds shows a large spread, with the majority of finds sloping between 5 and 25°.

The penetration of the large roots terminates at the top of the LC-MSA Lower, while micromorphology shows that some smaller roots continue into the LSA-MSA Lower, suggesting the conditions of the LC-MSA Lower at the time of root formation were less agreeable to root formation. This could be due to increased water content in the LC-MSA Lower, a very dense artifactual component, high organic content, or a combination of all three creating a supersaturated environment.

There is an OSL age (111402) of 125 ± 5 ka, suggesting that the LC-MSA Middle accumulated at the transition between MIS 6 and MIS 5e, making this a rare deposit in coastal South Africa. The presence of shellfish would suggest that it dates to the latter part of this transition, after the sea transgressed sufficiently to bring the coastline within 5–10 km. The adjusted maximum and minimum ages are 130 and 120 ka, respectively.

LC-MSA Upper The LC-MSA Upper caps the anthropogenic facies and is a heavily cemented zone composed of multiple layers. Micromorphological observations document several phases of cementation. The cementation events postdate the deposition of the layers in the LC-MSA and stabilized and hardened both the LC-MSA deposits and at least two aeolian dunes that sealed the deposits below, and in the latter case, the entire cave entrance (see discussion below). Lithic artifact densities continue to decline from the layers below, as does the mean MS, suggesting an overall decrease in occupation intensity (Fig. 7). There is a slight preferred orientation to the finds, and the micromorphology suggests this may be due to a combination of aeolian activity, very low energy water flow (such as dripping water), and gravity.

Within the LC-MSA Upper we recognize three layers:

1) A lower, very hard sandy and silty layer that directly contacts and transitions into the richer archaeological deposits of the LC-MSA Middle. This layer includes multiple lenses of black to dark brown organic material.
2) A sandy horizon (weighted mean OSL age of 126 ± 4 ka) with a lens of shellfish (Fig. 8). This horizon is well preserved in the northern section and in the Northern area of the LC-MSA generally, but is eroded off the southern portion of the LC-MSA in the main area of excavation. It must have been deposited prior to the sealing of the cave by the dune and included significant organic activity as indicated by the black lenses. Micromorphology also documents the presence of small to

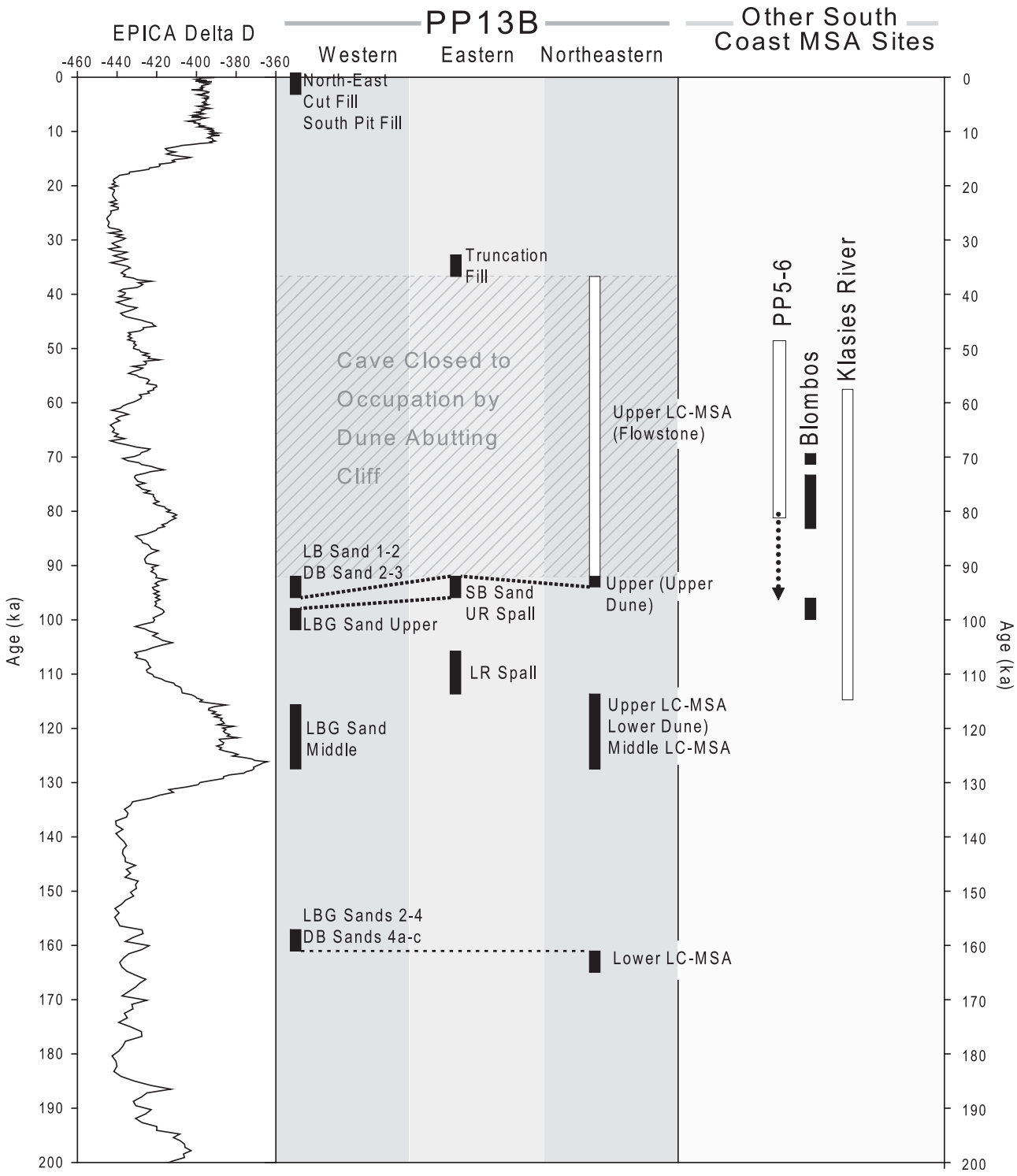

Fig. 6. The age of occupations at PP13B relative to global climate as reflected by EPICA δD record (EPICA Community Members, 2004) compared to several other important south coast sites. Age spreads of other sites include PP5-6 (currently under excavation by the SACP4 project; Brown et al., 2009), Blombos Cave (Henshilwood et al., 2002, 2004; Jacobs et al., 2006, 2008), and Klasies River (Deacon and Geleijnse, 1988; Deacon, 2001; Jacobs et al., 2008).

larger fragments of shell, and some show slight rounding suggesting potential movement. The adjusted maximum and minimum ages are 133 and 115 ka, respectively.

3) A capping dune (weighted mean OSL age of 93 ± 4 ka) that covered the LC-MSA and closed the cave to human occupation. The surface of this cemented dune is visible on the north wall of the cave as a steeply sloping remnant of the leeward face of the dune, and this same sloping leeward dune surface is preserved in nearby PP13A. The PP13B leeward face has a lip of flowstone stratified on top of the dune surface, which likely formed after the closure of the cave. One way to explain this is that the dune formed, was vegetated near the opening and fixed, cemented, and then eroded. Micromorphology shows that cementation of the upper crust of this dune is a result of the vegetation, not

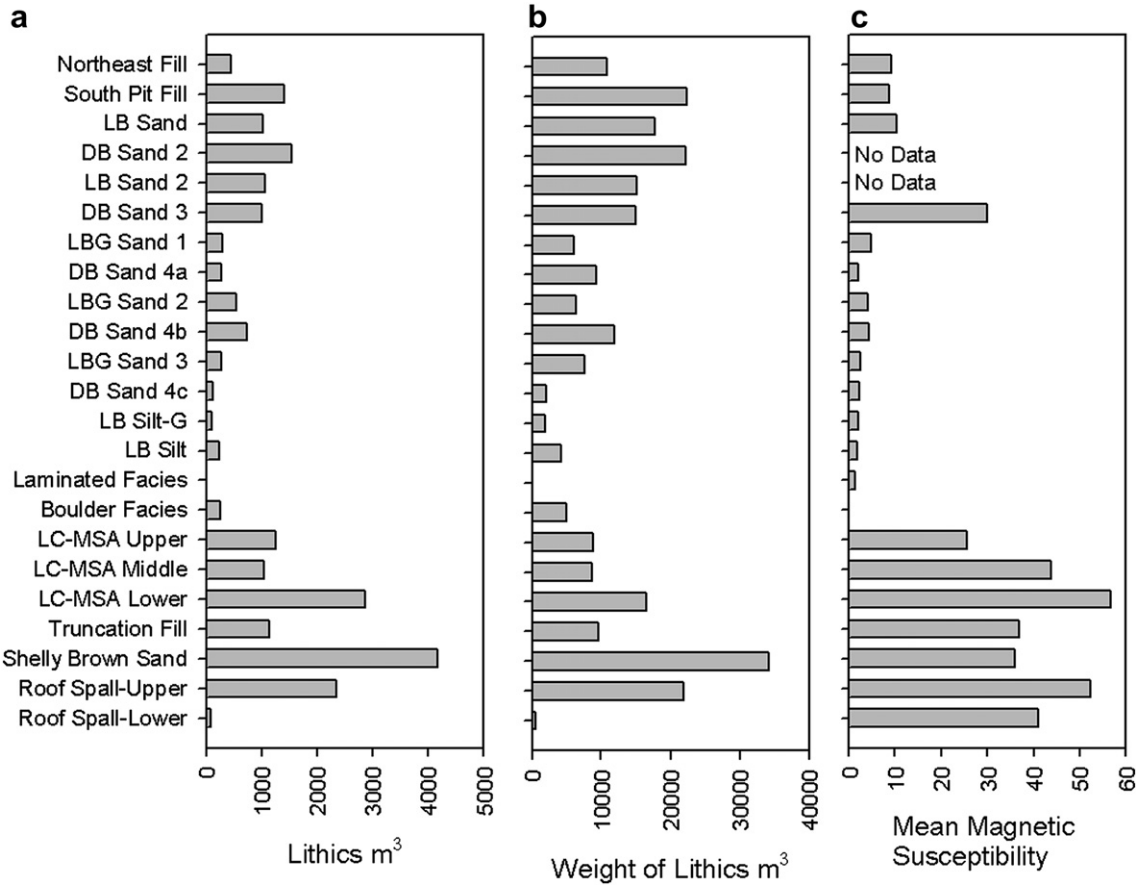

Fig. 7. For each stratigraphic aggregate (a) the number of lithic artifacts per m^3, (b) the sum weight (g) of lithic artifacts per m^3, and (c) the mean magnetic susceptibility.

saturation of the entire dune. The adjusted maximum and minimum ages are 98 and 91 ka, respectively.

LC-MSA Flowstone The LC-MSA Flowstone drips from the cave wall and over the LC-MSA sequence where the LC-MSA abuts the cave wall. It grew between ~92 and 39 ka as aged by six U–Th samples (Fig. 6; SOM). The U–Th age of ~92 ka is concordant with the weighted mean OSL age of 93 ± 4 ka on the sands above and shows that speleothem formation commenced directly after closure of the cave by the dune. The U–Th ages also provide a precise minimum age estimate for the sediment samples from below collected for OSL. At its thickest the flowstone is about 5 cm of laminated brown to yellow flowstone.

Our 2005–2006 excavations did not reach the area where the flowstone is present, so we core sampled approximately 50 cm to the north of the excavated northern LC-MSA profile, pushing the core sufficiently deep to sample the entire sequence of sands and lenses in the LC-MSA Upper. This core was prepared into a micromorphology sample (46579), and study of this sample shows this flowstone cap directly on the aeolian sand of the LC-MSA Upper (Fig. 8). The contact is a rough and wavy microscopically sharp boundary with the underlying LC-MSA Upper and penetrates and seeps into it at various locations. This contact definitively documents the LC-MSA Flowstone stratigraphically overlying the top of the LC-MSA Upper.

We have developed a 3D model of the dune configuration and the flowstones and it shows that cave was mostly closed between ~92 and 39 ka. While the flowstone is predominantly sand free it does contain growth lines and inclusions of aeolian sand, suggesting that during the period of formation there were some openings to the outside. Carbonaceous layers cemented to the north wall (micromorphology samples 46557 and 46552) are not archaeological, but have significant amounts of gypsum and black organic phosphate rich material that is likely guano, also suggesting that bats or birds could have entered during this partial closure.

Western area

The Western area was excavated in each of the seasons except the October 2005 season. Following the test excavations of 2000, we began an excavation slightly to the northwest of the test, in the hope of encountering the previously sampled upper layers in a less disturbed area and perhaps with thicker deposits since the sediments sloped up rather abruptly. Since the stratigraphy of the 2000 test was simple (just one archaeological layer) and thin (just 20 cm), we expected that excavating in a fairly horizontal manner, peeling layers back one by one, would be effective.

However, after several weeks of excavation we failed to encounter any stratigraphy that remotely resembled that in the test just 2 m southeast. The MSA deposits were much thicker than those encountered in 2000, and it was clear that there must be a major break in stratigraphy across the short gap between our 2000 and 2003 excavations. We stopped to re-evaluate strategy and focused on horizontally small excavations to the base of the deposits to create numerous sections so as to control for the complicated stratigraphy. The sediments thickened from approximately 20 cm of archaeological sediment to nearly 1 m from the N98 to N98.5 line, and there were numerous disturbances, explaining the lack of resemblance between the 2003 sediments and those revealed in 2000.

Table 2
The amount of sediment removed, count of lithic artifacts, weight of lithic artifacts, density of lithic artifacts, and average magnetic susceptibility for the stratigraphic aggregates at PP13B[a]

Stratigraphic aggregate	m^3 of sediment	Count of lithics	Sum weight of lithics (g)	Lithics m^3	Lithic weight (g) m^3	Average magnetic susceptibility
Western area						
Northeast Fill	0.067	30	722	450	10,828	9.24
South Pit Fill	0.033	46	730	1406	22,339	8.66
LB Sand 1	0.324	330	5773	1019	17,838	10.45
DB Sand 2	0.145	224	3243	1540	22,298	ND
LB Sand 2	0.051	54	768	1061	15,104	ND
DB Sand 3	0.472	472	7089	999	15,007	30.01
LBG Sand 1	0.746	212	4559	284	6107	4.74
DB Sand 4a	0.044	12	404	274	9244	2.18
LBG Sand 2	0.049	27	312	547	6326	4.15
DB Sand 4b	0.046	34	549	738	11,926	4.45
LBG Sand 3	0.007	2	56	269	7606	2.50
DB Sand 4c	0.134	15	271	111	2018	2.25
LB Silt-G	0.188	19	348	101	1850	2.03
LB Silt	0.204	48	846	236	4154	1.85
Laminated Facies	1.177	17	63	14	54	1.27
Boulder Facies	0.148	37	746	250	5027	ND
Northeastern area						
LC-MSA Upper	0.047	58	415	1246	8909	25.66
LC-MSA Middle	0.172	179	1508	1038	8745	43.84
LC-MSA Lower	0.532	1524	8806	2863	16,543	56.76
Eastern area						
Truncation Fill	0.410	468	3960	1142	9661	36.87
Shelly Brown Sand	0.095	394	3243	4165	34,287	35.93
Upper Roof Spall	0.518	1213	11327	2342	21,869	52.45
Lower Roof Spall	0.548	41	313	75	570	40.97

[a] These data are used to develop Figure 7.

Overall, this Western area deposit appears from field observations to resemble a midden or dump compared to deposits excavated in the Eastern area of the cave. However, micromorphology does not provide support for this in the form of sediments that appear "dumped"—rather, combustion features appear to be *in situ*. With the exception of DB Sand 3, mean MS is rather low in the Western area, while lithic artifact densities vary between moderate to high. Marine shellfish are for the most part low in density to absent and micromorphology does not suggest that it was removed by dissolution.

Micromorphological observations fail to identify any significant turbation from burrowing insects or mammals, although at the surfaces of the sediments there is evidence of the attack on the roof spall by mites. This might be a significant process in the breakdown of roof spall into finer-grained sands. The sediments vary dramatically between those with strong anthropogenic signatures and those that are more or entirely geogenic. There are areas where there has been substantial geogenic disturbance by faulting, slippage, or subsidence, and MSA anthropogenic disturbance primarily from cutting and pit digging. There has also been modern disturbance in at least one area.

Boulder Facies The Boulder Facies is the base of the unconsolidated sediments as currently sampled and consists of a set of large rounded boulders at the base of the sediments, and the sediments between and around the boulders. It is not shown in any of the figures here, but can be seen in Marean et al. (2004: their Fig. 16). The only square and quads brought to this depth to date in the Western area are N97E97 NW, SW, and SE.

There is a thin rind of silty loam and clay found between and around the boulders, and some large open spaces around and on top of the rocks, possibly formed by water action at the contact of the rocks and the sediments above. This is also likely the source of the subsidence of many of the overlying sediments that is discussed below and illustrated in Marean et al. (2004: their Fig. 16). It included some roof spall but was otherwise sterile. This is a cobble beach formed by high sea levels.

Laminated Facies The Laminated Facies is the thick series of sediments at the base of the archaeological sediments throughout the Western area (Fig. 10). It directly overlies the Boulder Facies as observed in N97E97 in Marean et al. (2004). This is a predominantly sterile zone (Fig. 7) of grayish-brown sediment with thin multiple laminae of sand and silt, and intercalated yellow-brown spots and stringers. Micromorphology identifies the yellowish-brown features as guano and also identifies small amounts of micromammal bone. Micromorphology of the sands identifies them as breakdown products of the roof, not aeolian sand. This suggests that either the cave mouth had an obstruction that hindered the penetration of aeolian sands, or wind conditions were inappropriate for moving sand to the back of the cave. In thin section the sediments suggest a regular wetting of the deposit at the base, with a tendency to drier conditions and aeolian reworking at the top.

The few finds were mostly small pieces of fossil mammal bone that exhibit a polished surface. There was a very little roof fall. Finds from overlaying sediments penetrate down into it near the top. It is ~1 m thick as indicated by the one excavated square (N97E97) where we reached the boulder beach at the base of the deposits. The sediments are more distinctly bedded at the base. This facies is best interpreted as a low energy water lain deposit, an interpretation consistent with a seep in the back of the cave. Micromorphology sample 46563 penetrates into the Laminated Facies near the bottom of the sample and shows laminations of silty sandy sediments and guano. Above this there is a trend toward more terrestrial and dry sediment (LB Silt) with guano occurring as crumbly brown crusts and then a return to laminations and sorted sands. It is cut by at least one fault or slumping event that is clearly recognized in the north and west profiles of N97E97 in Marean et al. (2004: their Fig. 16). In Marean et al. (2004) the Laminated Facies was named the Ponding Facies, as we thought the laminated nature of the sediments suggested ponding. The micromorphologic analysis shows that this is not the case.

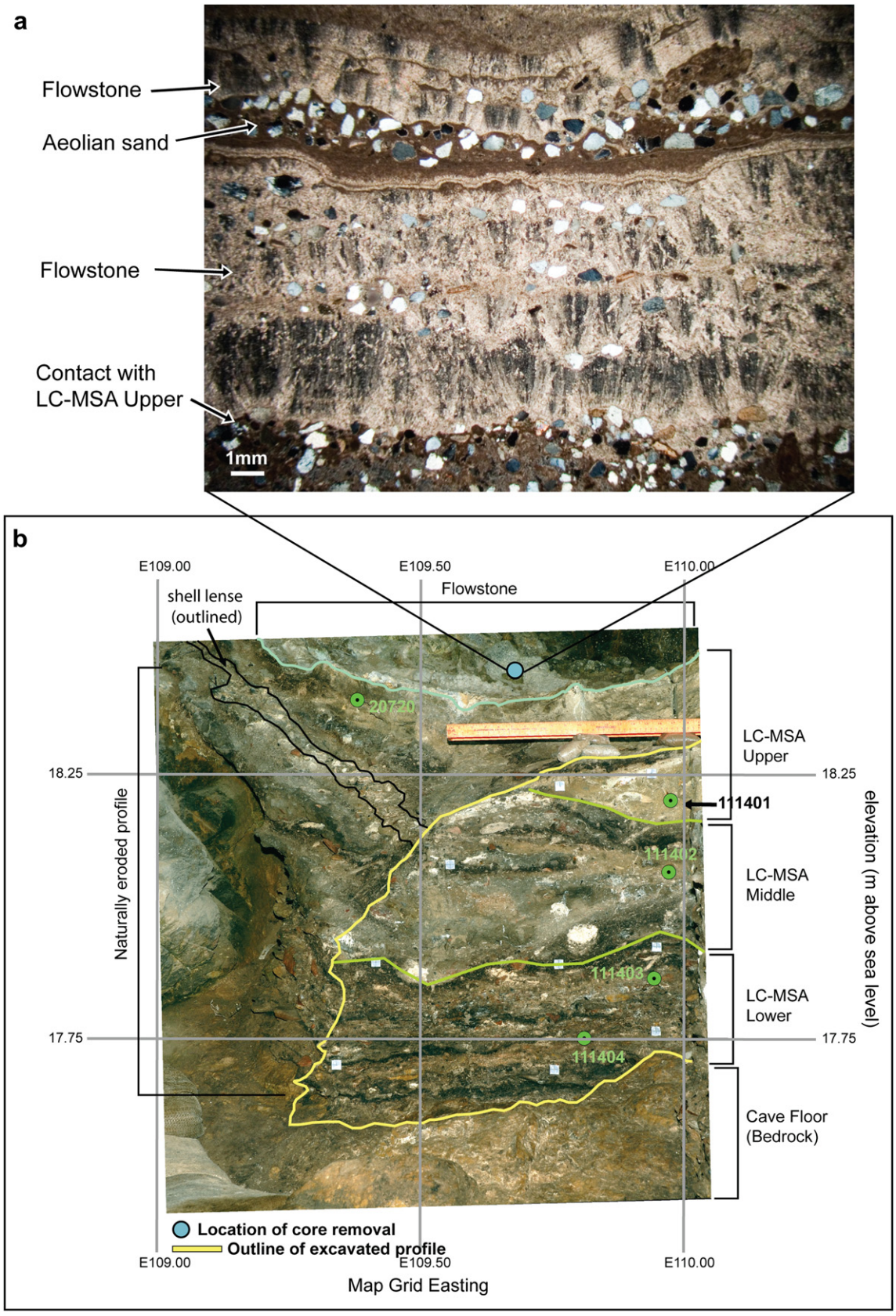

Fig. 8. N95.5 line Northeastern (LC-MSA) area north section photograph (rectified). (a) Micromorphology photograph of contact between flowstone and LC-MSA Upper dune, and (b) north section photograph of LC-MSA and contact of flowstone with LC-MSA Upper from E109 to E110. Note that the yellow lines only show stratigraphic contacts of the excavated section. The LC-MSA Upper extends back, as indicated by the black brackets.

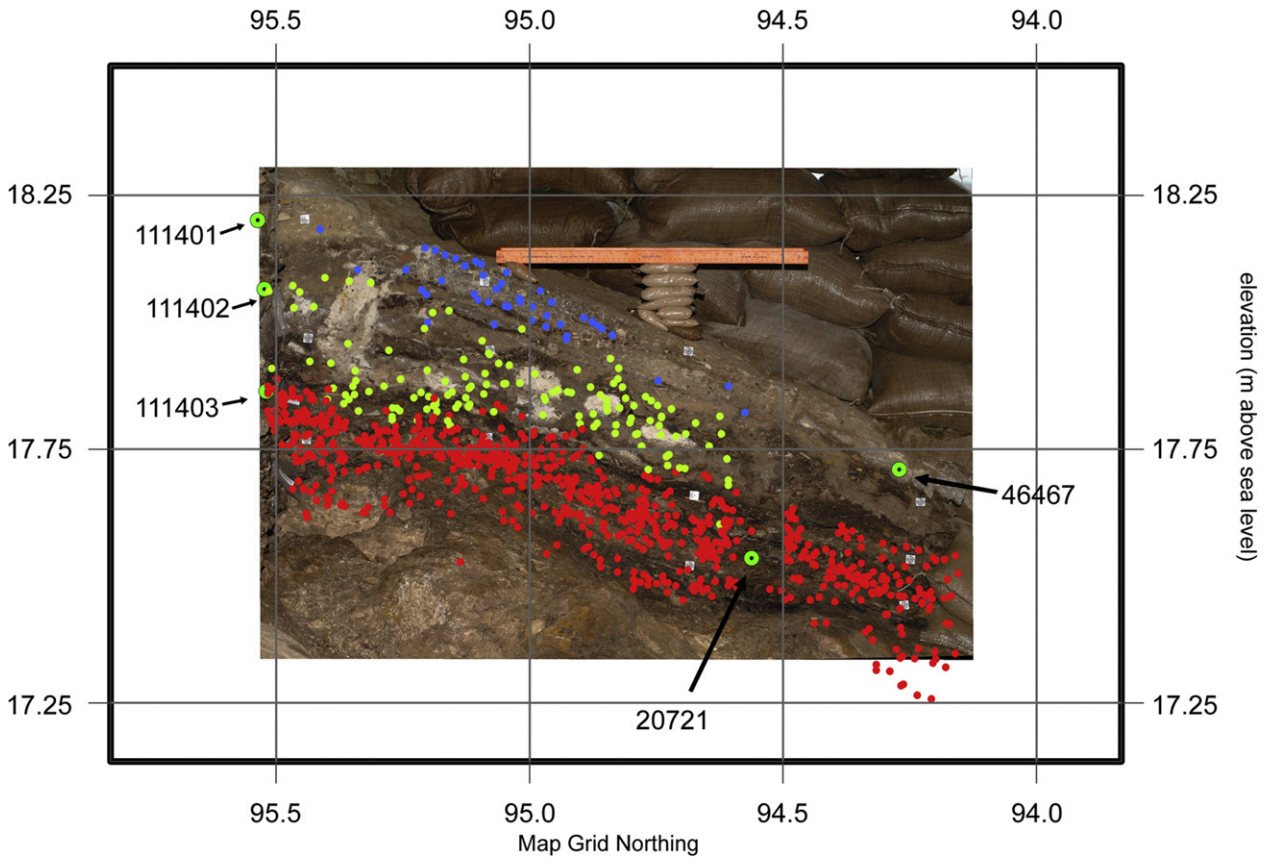

Fig. 9. E110 line Northeastern (LC-MSA) east section photograph (rectified) from N95.5 to N94.15 showing major stratigraphic aggregates as indicated by plotted finds and position of OSL samples. Red = LC-MSA Lower, light green = LC-MSA Middle, and blue = LC-MSA Upper.

There are three TT-OSL ages (samples 20724, 20730, and 20735) with a weighted mean age of 385 ± 15 ka, with adjusted maximum and minimum ages of 414 and 349 ka, respectively. This is concordant with an MIS 11 age for the formation of the sediments and is consistent with the interpretations that suggest a relatively higher land surface and sea level at the time of formation.

Light Brown Silt Facies The Light Brown Silt Facies (LB Silt) was originally defined as the erosion gulley facies in the 2000 excavations (Marean et al., 2004). In the 2000 excavations, the entire excavated material fell within the zone of disturbance that has the profile of a gully, hence our name for the layer. However, as we expanded the excavations laterally to the north and west we discovered that this layer continues laterally nearly throughout the excavated area (Fig. 10), thickens appreciatively, and loses its "gulley" character. We have decided to rename it as LB Silt as it transitions out of this slumped area and LB Silt-G (for gulley) in the area of the gulley. In the area of the slumping, there is some mixing of this layer with materials above and below, but we were fairly successful at following in excavation the slumped layers. The materials in this sediment are most likely displaced downward.

Micromorphology identifies the LB Silt as poorly sorted silty sand with significant apatite input from guano. Near the top of the layer there is evidence of a stabilizing surface and increases in organic input that leads to the archaeological layers. The majority of the finds have slope lines between 0 and 20°, with the 10–15° being the most well-represented group, and this appears to follow the slope of the stratigraphy. Some finds are sloped much more steeply, but this is randomly spread as opposed to clustered and thus likely represents only local disturbance. Lithic artifact densities and MS are low and comparable to the Laminated Facies (Fig. 7).

OSL sample 46456 is from the N99 line section (Fig. 10) at the base of this facies and it is saturated. From the southwest of the excavation is sample 46461, taken from the E95 line profile at the top of this facies near the boundary with the base of LBG Sand, has an OSL age of 157 ± 8 ka. The adjusted maximum and minimum ages are 349–152 ka, respectively, with the upper age range established by the age of DB Sand 4b (see below).

Dark Brown Sand Facies The Dark Brown Sand Facies (DB Sand) is a series of horizons that are defined by their dark greasy brown sandy characteristics. They have lighter brown to gray sandy horizons between them. There are low to moderate densities of lithic and faunal finds, and the dark nature of the material suggested in the field that they may be burned; the MS analysis is consistent with this (Herries and Fisher, 2010). Micromorphology shows that all these sediments, along with LBG Sand, have strong input from aeolian sand from the beach zone, while there continues to be significant input of guano.

The DB Sand 4 are a set of dark brown lenses stratified within the LBG Sands (Figs. 10 and 11) and 4c is at the base. The DB Sand 4 series is cut and disturbed in several places, and given that all are thin, they blend together in the disturbed areas. Further to the northwest they retain their integrity, and in the southwest one can still clearly see them warped but discrete directly in the center of the fault shown in Figure 17 of Marean et al. (2004; N98 Line Section between E96.5 and E97).

Lithic artifacts and fauna are present in the DB Sand 4 and show a slight increase relative to the underlying areas, but MS remains low (Fig. 7). We found in DB Sand 4a numerous skeletal elements of large animals (size 4) clustered with several hammerstones. The slope line lineations vary widely between the DB Sands. DB Sand 4a

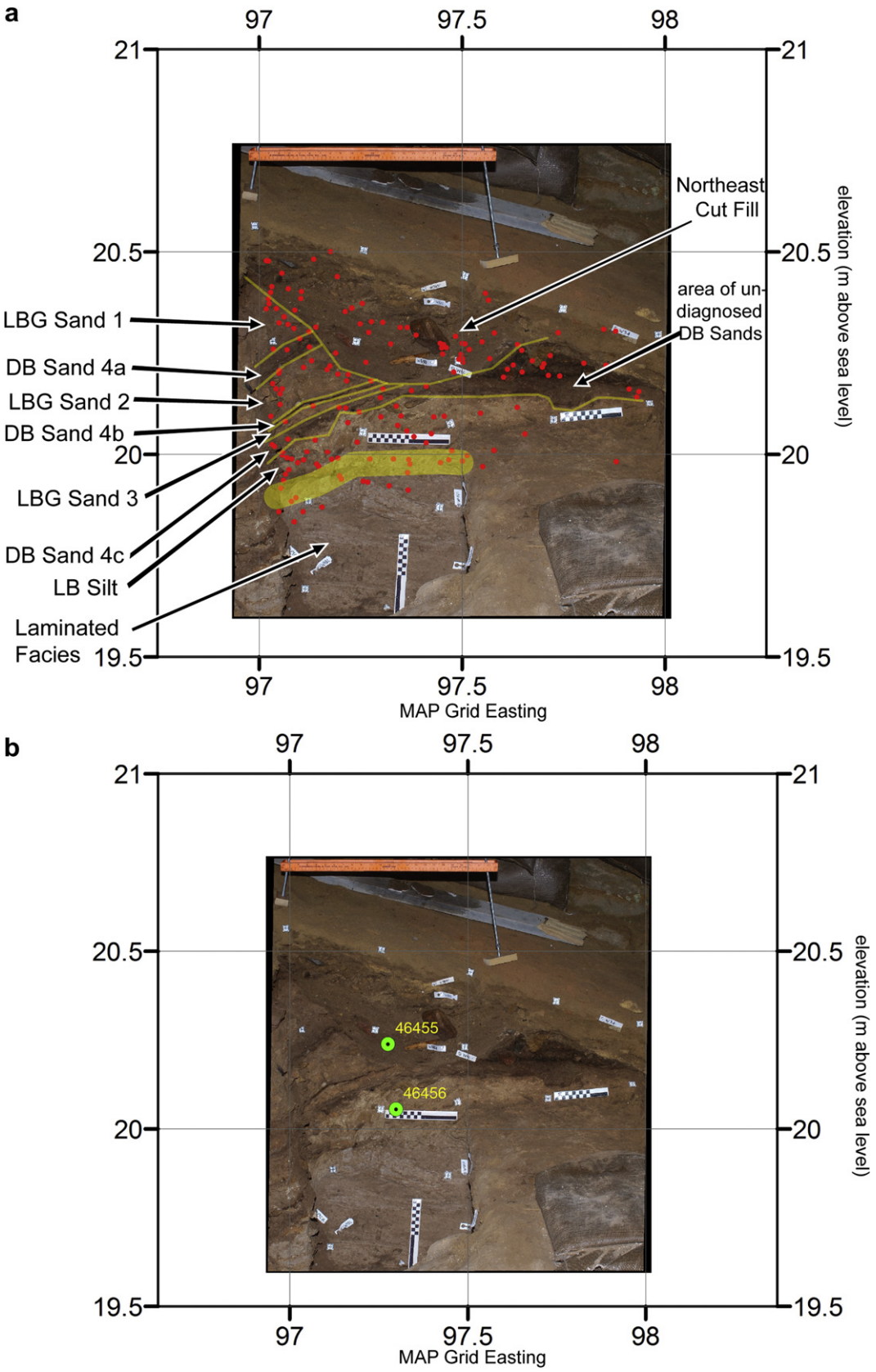

Fig. 10. N99 line Western area north section photograph (rectified) from E97 to E98. (a) The section photograph showing the major stratigraphic aggregates and the distribution of lithic artifacts (red dots) from a 25 cm north-south slice, and (b) the section photograph showing the location of the OSL samples taken from this section.

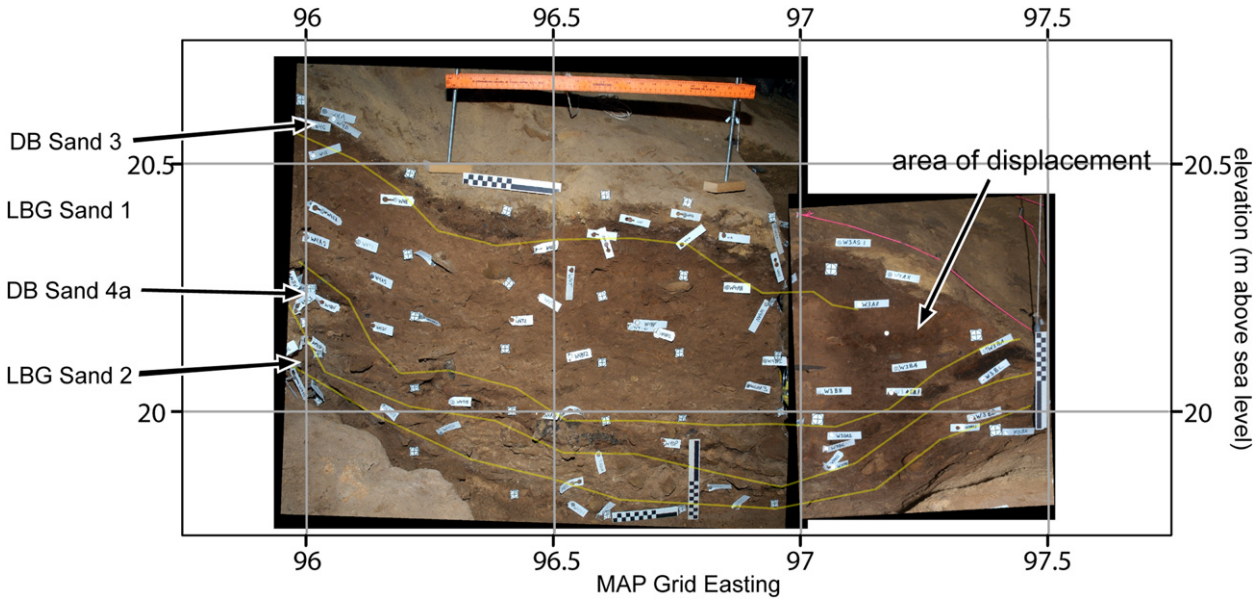

Fig. 11. N98.5 line Western area north section photograph (composite rectified) from E96 to E97.5.

is dominated by slope lines between 0 and 10°, while there are several specimens that are nearly vertically sloped. DB Sand 4b has more specimens between 10 and 20°, and few more vertically oriented. DB Sand 4c resembles DB Sand 4b in slope. These thin lenses of dark organic material are best seen in the N99 Line section (Fig. 10), the N98.5 Line section (Fig. 11), and the E97 Line section (not illustrated here). DB Sands 4a and 4b are cut by a disturbance that may be anthropogenic (Northeast Cut Fill), the fill of which is dated to the late Holocene, and around E97.50 of the N98 line DB Sands 4b and 4c nearly blend together. However, to the west all three are separated by thin lenses of lighter brown sandy sediment that is less organic (LBG Sands 2 and 3; Fig. 10).

Micromorphology sample 46563 extends across DB Sands 4a, 4b, and 4c. DB Sand 4c shows a surface of decayed organic matter that must have been exposed for a significant time, and thus was likely a living surface. DB Sand 4b samples the first real charcoal and burnt bone layer in the western sediments. DB Sand 4a displays abundant charcoal and is clearly an *in situ* burning feature. So far it is the lowest occurring archaeological feature that is documented by micromorphology to be burned *in situ*.

DB Sands 3 and 2 are stratified above LBG Sand 1 (see below) and are within LB Sand 1. They are not disturbed by the subsidence events, but rather drape over the slumped surface of LBG Sand 1 and present a clean contact with it that likely represents an erosion event. DB Sand 3 is the dark greasy horizon that includes the dense MSA material equivalent to Brown Sand MSA Facies in the 2000 excavations in N97E97 (Marean et al., 2004). However, excavations in 2003 expanding to the north and west revealed at least two separate lenses of dark organic material (DB Sands 2 and 3) that join near the East 95.60 line of the North 97.00 line. Originally we distinguished a DB Sand 1, but it is clear that it is indistinguishable from DB Sand 2 and the term is dropped.

DB Sand 3 is one of the most prominent layers in the western excavations—it stands out visually with its dark color and is laterally extensive, being found nearly throughout the excavated area. It functions as a major stratigraphic boundary in several ways. First, it is underlain nearly throughout the excavated area by the much lighter LBG Sand 1. And second, below it there was a major disturbance by what was most likely a subsidence or slippage discussed above, as well as at least one cutting event that is either anthropogenic or geogenic slump. DB Sand 3 drapes over this event and is separated from it quite cleanly. It also displays an increase in lithic artifact densities and increase in MS (Fig. 7).

Micromorphology sample 20222 is taken from the E96.5 line section, while 20296 is taken from the N98 line near E96.5. Both samples cover essentially the same sediments and incorporate a significant portion of DB Sand 3 at the bottom of the sample and a thin part of LB Sand 1 and surface sediments. DB Sand 3 in thin section is full of charcoal and burnt bone. Micromorphology sample 46564 samples DB Sand 3 further to the north of 20296 and documents significant amounts of charcoal and burning. The slope lineations of DB Sand 3 are highly variable, with slopes between 0 and 30° dominating the pattern, likely resulting from DB Sand 3 hugging the surface of the lower sediments, which as noted above are in various locations disturbed by subsidence or cut by anthropogenic activity.

There is an important temporal and stratigraphic distinction between the lower DB Sand 4 series (a–c) and the upper DB Sands 3 and 2. OSL sample 46458 is in DB Sand 4b and has an age of 159 ± 7 ka. The DB Sand 4 are stratified within the LBG Sands and there are three OSL ages from the LBG Sands that are stratified above the DB Sand 4 ranging from 127 ± 7 to 98 ± 4 ka. The DB Sand 4 series all are aged to MIS 6 given that the LBG Sands above them have two ages near the boundary of MIS 5e and 6, and DB Sand 4b has an OSL age of 159 ± 7 ka. U–Th sample 29807 from DB Sand 2 is aged to 102 ± 0.08 ka and provides a maximum age for it and everything above. So, while sedimentologically similar, DB Sand 4 and DB Sands 3 and 2 are from MIS 6 and MIS 5, respectively. The adjusted maximum and minimum ages for DB Sands 3 and 2 are 102 and 91 ka, respectively.

Light Brown Gray Sand Facies The Light Brown Gray Sand Facies (LBG Sand) is the lighter brown to gray sediments that are stratified between the Dark Brown Sands starting below DB Sand 3. We recognize a single LBG Sand, and then when the DB Sands 4a–c were encountered, we subdivided it into LBG Sand 2–4, with LBG Sand 2 below DB Sand 4a and so on. There are lenses of finds scattered through these sediments, but not as dense as is found in the DB series, and they are distinguished from the DB series in that they do not include the dark greasy sediments. Micromorphology (20222) shows that these are decalcified sediments of aeolian sand

with significant amounts of apatite, most likely from the input of guano. Micromorphology sample 46563 extends across LBG Sands 4 to 2 and shows that these are a mixture of roof spall and fine-grained aeolian sand and apatite with guano origin.

LBG Sand is one of the thickest and most laterally extensive layers, though it appears thin and discrete in the test excavations of 2000 where much of it was likely truncated off. It then thickens appreciably to the north and west; however, much of it is cut away in the SE quads of N97E96 by an MSA disturbance that predates the DB Sand 3. In N98.5 line section (Fig. 11) it is the thickest layer and is centered in the middle of the profile.

As with the DB Sand 4 series, the LBG Sands are also disturbed in several areas by subsidence and slumping. Slope line lineations between 0 and 30° are dominant, while there are some finds that are nearly vertically oriented between the E96 and E97 lines where the truncation appears, thus suggesting some very isolated disturbances. The contact between the LBG Sands and the overlying DB Sand 3 varies across the area from sharp, suggesting a geogenic or anthropogenic truncation, to more gradual and diffuse where a truncation is lacking.

There are two OSL ages where the contact with DB Sand 3 is sharp: 127 ± 7 (46463) and 122 ± 5 (46457). There are also two OSL ages where the contact with DB Sand 3 is not sharp: 98 ± 4 ka (46459) and 99 ± 4 ka (46464). This suggests that significant amounts of the LBG Sands may have been removed by the truncation where the contact is sharp. So far we have ages only on those above the DB Sand 4 units. The adjusted maximum and minimum ages for LBG Sand are 134 and 94 ka, and it is very probable that there are two separately aged units present that we have yet to define chronometrically.

Light Brown Sand Facies The Light Brown Sand Facies (LB Sand) is the light brown material below the surface that includes substantial MSA finds, but is above the dark greasy horizons of DB Sands 2 and 3 (Fig. 12). Its lithic artifact densities are high but MS is lower than DB Sand 3 (Fig. 7). It occurs in the Western and Northern areas of the excavation, but is absent in the Southeastern areas

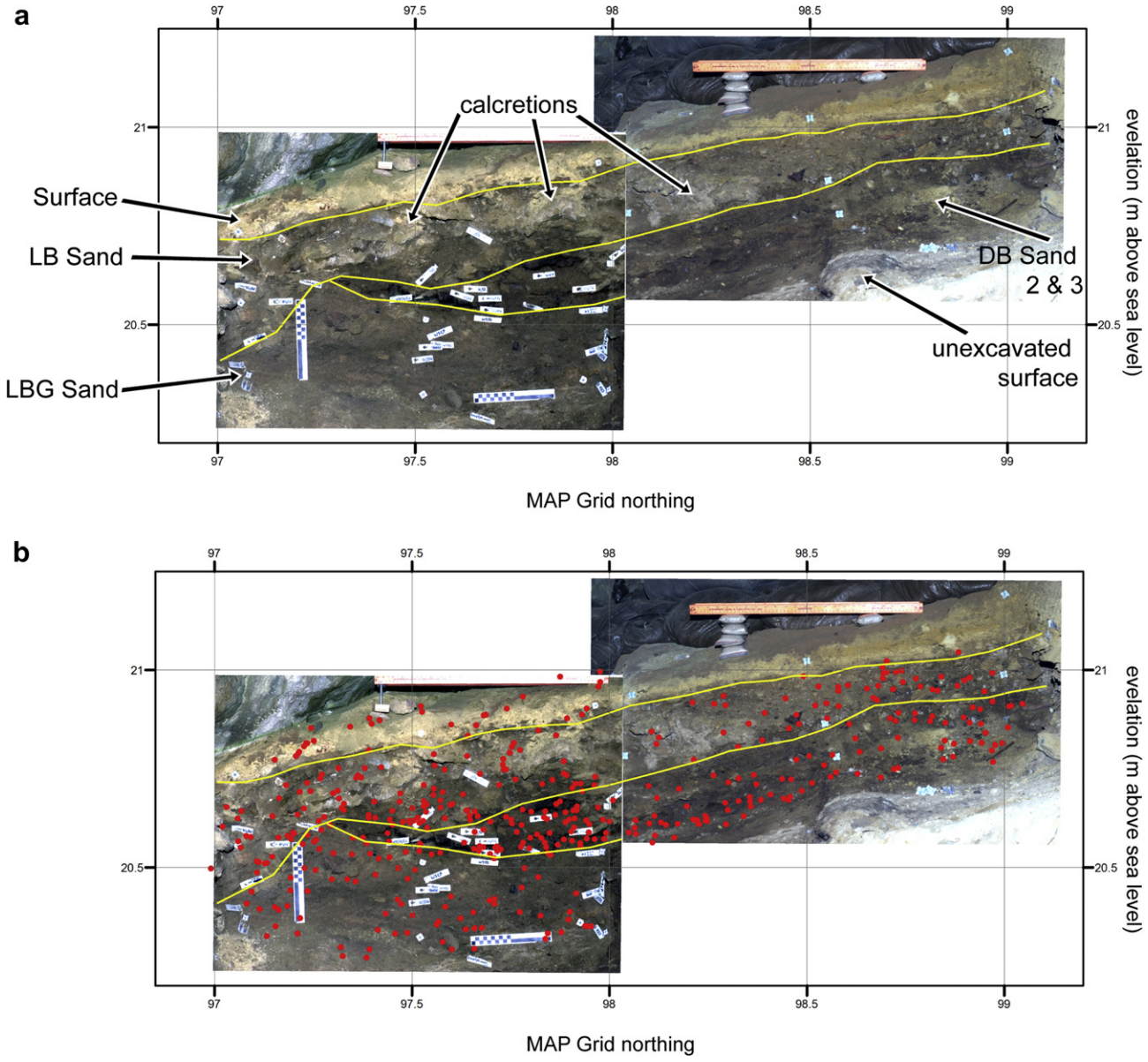

Fig. 12. E95 line Western area west section photograph (composite rectified) from N97 to N99. (a) The section photograph showing the major stratigraphic aggregates, and (b) the section photograph showing the showing major stratigraphic aggregates and the distribution of lithic artifacts (red dots) from a slice from 25 cm slice.

where it is both cut away by disturbances and thins out. It is coarse grained with substantial amounts of roof fall that concentrates in size between 1 and 5 cm long, but also includes subcentimeter platy roof spall that micromorphology shows has been attacked by mites. Slope line lineations of plotted finds are variable and abundant between 0 and 25°, while in the area between E95.5 and 96 there are many specimens that are nearly vertically oriented, suggesting some disturbance in this area.

OSL sample 46460, which is above DB Sand 3 in the middle of this facies, has an age of 90 ± 4 ka. Sample 46462 from the N97 section just above DB Sand 3, in the lower part of this facies, has an age of 90 ± 4 ka. U–Th sample 27357 is aged to 94.7 ± 1.1 and provides a maximum age for it and everything above. The adjusted maximum and minimum ages are 94 and 91 ka, respectively.

South Pit Fill The South Pit Fill is loose fill sediment in a pit clearly visible in the N97 line south section, near the E96 line (not illustrated here). The fill appears to be MSA in age, and the plotted finds are for the most part sloping between 0 and 10°.

Northeast Fill The Northeast Fill is the light brown loose sandy sediment found in the pit or gulley clearly visible in the N99 line section between E97 and 98 (Fig. 10). It thickens appreciably to the north, until in the northern section of N99 line it is nearly 50 cm thick. There is some roof spall in it, as well as low amounts of MSA lithic artifacts that must have been transported in and are out of context. The finds have a widely variable slope lineation, with a concentration in the 20–25° range, and numerous specimens are nearly vertical. Most of the finds slope down to the west with the sediment dip.

This was deposited after the fault or slump that runs through N98E97, an event that resulted in the sediments to the west displacing downward. This material then either slumped down into a depression or was deposited there during the normal course of sedimentation. The clean truncation of LB Sand 1, DB Sand 3, LBG Sand 1, DB Sand 4a, and LBG Sand 2 suggests that the Northeast Fill filled an eroded surface. OSL sample 46455 is from the lower part of this facies, has an age of 2.3 ± 0.3 ka, and suggests that the filling episode, if not the disturbance, is a relatively recent event.

Surface sediments This is excavated material from the surface. These are yellowish to brown surface deposits that have been trampled during modern times and consist primarily of coarse matrix of roof spall material. Micromorphology sample 20222 shows that the surface sediments include roof spall that is eaten by mites and significant amounts of dissolving carbonate grains.

Eastern area

The Eastern area was excavated during each of the seasons. In 2000, we excavated one square meter as a test, and the sediments were very thin (Marean et al., 2004). South of the N92 line, only three distinct stratigraphic aggregates were recognized: surface sediments, Re-Deposited Disturbance, and Roof Spall Facies. In 2003 and 2004, we excavated several square meters of deposit from the N91 line to the N93 line. The archaeological layers were thin and often cemented in patches, but hearths and lenses of archaeological material were well preserved, often hugging the boulders at the base of the deposit. In the more southern area of the deposit, there is a tendency for the archaeological deposits to be tucked into valleys in the bedrock depressions at the base of the deposits.

In that area, we excavated with a strategy aimed at following layers horizontally and exposing the isolated hearths laterally, often having numerous quads open for excavation. This was possible due to the relative horizontally continuous distribution of the layers and the rarity of major disruptions to that stratigraphy, unlike in the Western area. Much of the excavated area south of the N93 line was so thin that sections were never thicker than 20 cm. The sediments to the south were thin, as we would learn, due to the erosion of sediments off the top. Excavation was slow due to the regular cemented patches (from roof drip) that were encountered. Micromorphology suggests that this cementation stage was late in the formation of the sediments, probably after much of their deposition. Micromorphology did not identify any significant turbation from burrowing insects or mammals.

As we approached the N93 line in our excavations, the deposit began to thicken and discrete lenses started to be clear. When we reached the N93 line we began to excavate in a single east to west oriented line into the northern section so as to preserve a long east to west-oriented section. In 2005, we approached the N93.5 line and suddenly the deposits thickened appreciably (Fig. 13) with multiple layers being observed in the northern section. Importantly, a distinct truncation was seen near the N93.5 line in the western section. This truncation, caused by an erosion event that cut through this area and evidently removed a significant portion of sediment from the top of the area south of the N93 line, is the likely cause for the thinness of the archaeological deposits to the south.

Bedrock The Bedrock is at the base of the sediments as currently sampled and consists of round and polished TMS, sometimes fractured and fresh. Smaller cobbles of roof fall are common on top of and between the larger undulating bedrock surface. This is the base of the cave, and it is likely that much of the rounding was caused by high sea levels.

Lower Roof Spall Facies The Lower Roof Spall Facies is at the base of the excavations stratified on top of the bedrock and is an MSA horizon that is primarily clast supported matrix of small (1 cm and smaller) roof spall with fresh edges in the south, to a more sandy deposit in the north. Within it are cemented patches and this is more common in the more southerly parts of the excavated area. The deposits are tucked between the bedrock and form a thick fill between them, and then thin out if they extend over the top of the boulders. Archaeological finds are rare and concentrated near the top, but MS values are high (Fig. 7). Slope line lineations concentrate between 0 and 15° and closely follow the surface of the bedrock. Micromorphology shows that there are fragments of aeolianite in the cemented areas that resemble the aeolianite that overlies the LC-MSA.

There is some flowstone at the base of the sediments that may be very ancient and derive from a pre-MIS 6 cave closure event that also is suggested by two detached flowstone pieces (47013 aged by U–Th to 307 ± 11 ka and 47014 at equilibrium) found in the surface sediments. OSL samples 46496 and 46741 both have ages of 110 ± 4 ka. The adjusted maximum and minimum ages are 114 and 106 ka, respectively.

Upper Roof Spall and Shelly Brown Sand Facies The Upper Roof Spall Facies and Shelly Brown Sand blend together with the latter stratified above, and the OSL ages for the two overlap. In some areas we can separate them clearly (for example the western part of the N93.5 section), while in other areas separation is impossible (middle section of N93.5 section). In particular, at the E107.80 line on the N93.5 section there appears to be a disturbance, and it is impossible to follow the strata clearly from west to east. In this area there are several plotted finds that are oriented nearly vertically, as in the Upper Roof Spall Facies, and this is further evidence for a localized disturbance. For these reasons we have been conservative in lumping them together here, but in the reporting some authors have elected to analyze the finds separately.

The Upper Roof Spall and Shelly Brown Sand thicken appreciably from south to north. In the southernmost area it is a set of connected or isolated thin layers of burning, such as hearths, that become more complex and interlocking to the north. Stratified within this matrix are small, thin, well-preserved hearths with lithic artifacts and fauna laying in and beside the hearths. The

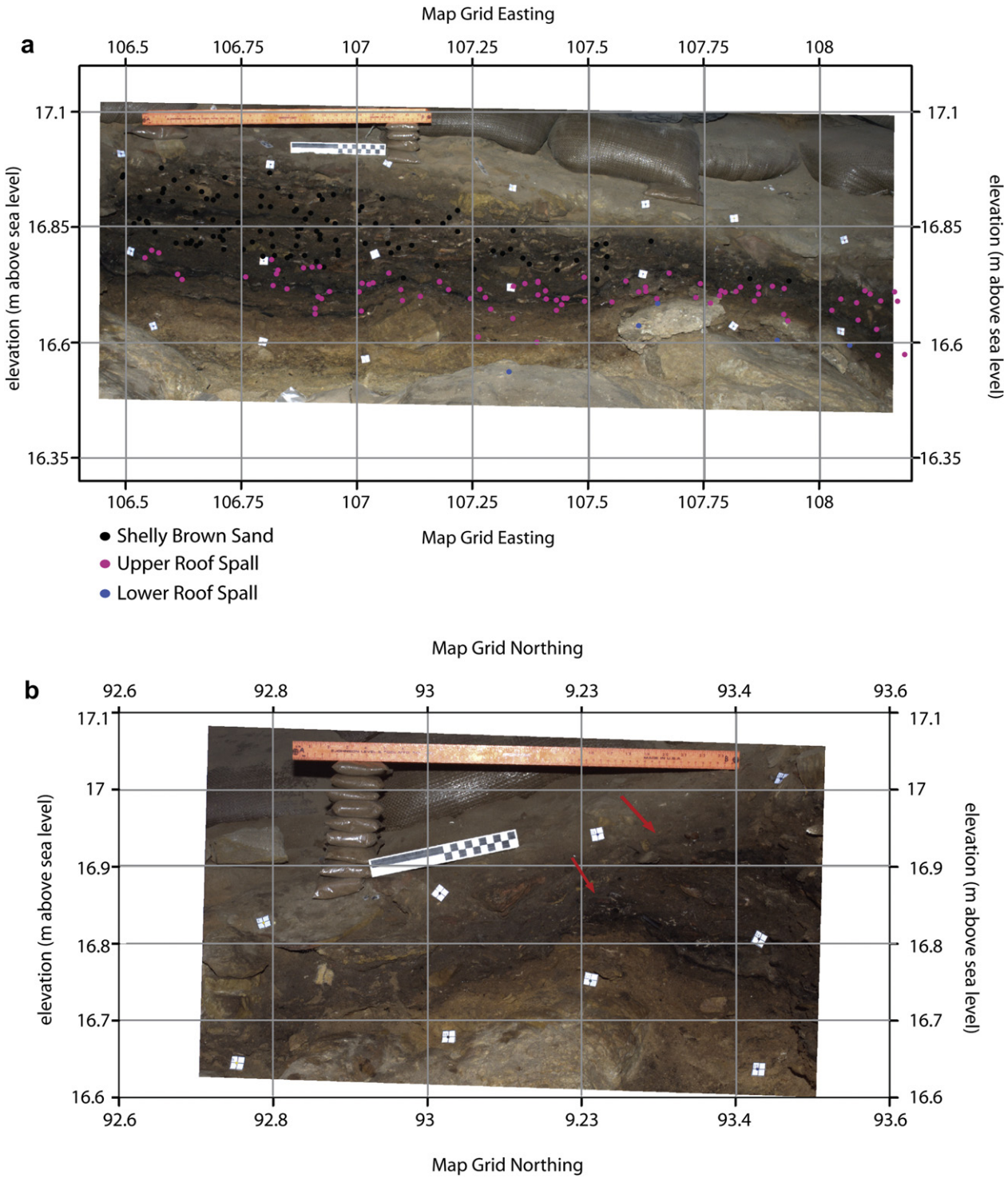

Fig. 13. Profiles from the Eastern area. (a) N93.5 line Eastern area north section photograph (rectified) from E106.5 to E108.25, and (b) the E106.5 line (rectified) from N92.8 to N93.5.

hearths have discrete bands of ash, charcoal, and baked (reddish-brown) sediment. These hearths appear as discrete units further to the south and then to the north bleed together into horizons of dark burnt material. Lithic artifacts, shellfish, and fauna are dense, while MS is high; and where we recognized the Shelly Brown Sand the shellfish component is particularly dense. Slope line lineations are most abundant between 0 and 10° and then decrease steadily in abundance between 15 and 30°. Very few are oriented vertically, but there is a concentration of vertically oriented artifacts around E106.5 in the Upper Roof Spall Facies and the Shelly Brown Sand from N92.5 to N93 that suggests a disturbance. To the south of the N93.5 line this facies was truncated, and it appears that south of N93 much of the top of this horizon was eroded off. In some areas, it was eroded all the way down to the Lower Roof Spall horizon.

We have six OSL samples scattered across the profile from the east and west, and only 46495 falls outside a rather tight cluster of ages. One U–Th age of a detached piece of speleothem is at equilibrium. Given that 46495 is so far outside the range of the other

OSL ages, we have excluded it here, and the adjusted maximum and minimum ages for the Upper Roof Spall Facies and the Shelly Brown Sand together are 98–91 ka, respectively.

Truncation Fill The Truncation Fill is the dark, rocky, organic rich horizon that sits directly atop the truncation at the top of the Upper Roof Spall Facies. It is seen at its thickest in the west section between the N93 and N93.5 lines. It is not present in the N93.5 section, as the truncation occurred south of that, but is first seen in the N93 section and terminates at the E108.20 line of that section.

Micromorphology sample 46523 spans part of the Truncation Fill, but misses the Re-Deposited Disturbance (see below). Micromorphology shows a flowing structure oriented at a steep slope of 45°. The truncation shows a shear plane across which the movement occurred. It is likely that this event was caused by gravity and some water. A possible explanation is regular sea spray wetting the deposits and causing slumping. The micromorphology shows that the Truncation Fill sediment is a remobilized MSA deposit, likely laid down roughly at the same time as the erosion event that planed off the top of the underlying deposits. Lithic artifacts and fauna are dense. The most abundant slope line lineations are between 5 and 10°, with substantial numbers between 10 and 15°.

The Truncation Fill is likely more recent than the MSA deposits below it. An AMS date on a charcoal sample taken near the boundary of the Truncation Fill and the Upper Roof Spall Facies provided an age of 35,340 ± 260 yr BP (GrA-23804), and may date the approximate age of deposition of the Truncation Fill. This could be consistent with the final U–Th age on the LC-MSA Flowstone (39.1 ± 0.4 ka), which likely represents the cessation of flowstone formation and thus the opening of the cave. This could mean that the massive erosion event indicated by the Truncation Fill was associated with the opening of the cave, followed by reoccupation by humans, as dated by the AMS age. We did not attempt to date the Truncation Fill with either TL or OSL as it was always near the surface and we were not confident of getting accurate dosimetry.

The Truncation Fill itself appears to have been partially eroded away to the west of the Eastern area, as it is not present in the western part of the N93 line section, but is replaced by and overlain by the Re-Deposited Disturbance. U–Th sample 57320 was dated at 84.3 ± 0.7 ka and provides a maximum age for the Truncation Fill and everything above.

Re-Deposited Disturbance The Re-Deposited Disturbance is a disturbed layer just below the surface. This layer includes modern bird feathers, modern artifacts such as cigarette butts, and the finds are nearly a lag deposit. We piece plotted one quad of this material and then, after determining that it was a modern disturbance, stopped plotting it. The slope line lineations are concentrated between 0 and 15° and some of the finds are oriented vertically. We believe that this material is re-deposited from the modern disturbance in the western excavations as the litter and spill of material from that area is traceable directly down into this area. It may represent other modern disturbances as well. U–Th sample 28773 was dated at 89.5 ± 0.7 ka and provides a maximum age for it and everything above.

Surface sediments The surface sediments are the same as those recognized in the western excavations and are self-explanatory. This is excavated material from the surface and is primarily a fine-grained ashy material in the eastern excavations, resulting from the tendency for modern fishermen to make their fires near the mouth of the cave, where in the Western area the surface sediments are lacking ash and are composed mostly of coarse roof spall. U–Th sample 27504 was dated at 43.8 ± 0.3 ka, sample 47013 at 307.2 ± 11.0 ka, and sample 47014 at equilibrium, thus providing evidence for a much older event of cave closure and speleothem formation.

Summary and conclusions

PP13B is a complex sedimentary trap with a long history of anthropogenic, biogenic, and geogenic input and erosion. The sea level highstand that formed the cave is unknown at this time, and at one time we thought it may be MIS 11, but that has recently been disproven through the application of several dating techniques. The earliest sediments are deposited at least by MIS 11, as measureable by our dating techniques, and the cave likely has an older phase as documented by the U–Th ages at equilibrium.

This long sedimentary history is preserved by a complex series of deposits that remain in rather modest vertical sections (rarely more than 1.5 m thick) scattered horizontally throughout the cave, seemingly unconnected stratigraphically. For this reason, our excavations targeted what we originally supposed to be the major areas of sediment preservation. However, due to the slow excavation technique and our desire to preserve large quantities of sediment for future scientists, connecting these is not possible. It is likely that the Western and Northeastern, and Eastern and Northeastern, sediments no longer preserve any stratigraphic connections. The relation between the Western and Eastern areas remains to be determined, and future work may help resolve their stratigraphic relations. In the text below we summarize the overall stratigraphic observations horizontally by area. We refer regularly to Table 1 and Figure 6, which provide our inferred sequence of the stratigraphic aggregates and their age ranges and temporal relationships.

Western area

The sequence in the Western area documents at its base in the Boulder Facies a high sea level that may be associated with the formation of the cave, but at least represents a high sea level that penetrates into the cave, at least as old as MIS 11. The Laminated Facies overlies this boulder beach and is separated from it by an erosion zone at the contact of the boulders and the Laminated Facies, and formed in a wet cave likely during MIS 11. There was little aeolian input with most of the sediments deriving from roof spall and decomposition of that roof spall. There was moderate stream activity, and the horizontally bedded sediments indicate that the landscape outside the cave at the time of formation must have abutted right up against the opening of the cave. A higher water table is indicated, likely near the elevation of the cave, perhaps in association with a high sea level. There is virtually no anthropogenic input, but there is significant avian input with potentially some small mammal input.

There is a sedimentary change at the transition from the Laminated Facies and LG Silt and sediments above. The overlying sediments have significant aeolian input, no evidence for stream action, significant but variable anthropogenic input (in the DB Sand 4 set of aggregates), continuing avian input, and subsidence and slumping of deposits likely derived from subsidence at the base of the Laminated Facies and during periods of deposition of the LBG Sands. The LBG Sands are sandy sediments with low frequencies of lithic artifacts and fauna, but stratified within them are dark bands of organic material with somewhat higher frequencies of lithic artifacts and fauna (DB Sands 4a–c). The DB Sands and LBG Sands that lie below the base of LBG Sand 1 date to MIS 6, and it is clear that DB Sand 4b and below date to early MIS 6. LBG Sand appears to have two separate depositional periods, one nearer to MIS 5e and another somewhat later near MIS 5c.

The most significant geogenic disturbance occurs in the more easterly areas of the western excavations, was described in the publication of the test excavations (Marean et al., 2004), and has been further delineated in the newer excavations. This is a slippage,

subsidence, or fault that runs from the middle of N97E97 north to northwest almost parallel to the western section of N98E97 or E97 line. This is clearly seen in Figures 16 and 17 of Marean et al. (2004) in the N98 line section drawing and photograph between E97 and E98. Sediments to the west slipped downward to the west, and the contact of the Laminated Facies and LB Silt became jumbled. All the sediments up to the top of LBG Sands were affected by this slippage, but the sediments of DB Sand 3 and above were not, and DB Sand 3 is tightly draped over the top of LBG Sands.

It is likely that this subsistence occurred in association with the MIS 5e high sea stand. We have analyzed tide gauge data from Mossel Bay and nearby Knysna from 1964 to 2003, and the highest tides in this area run up to 306 cm above orthometric zero, while mean tidal height runs at about +90–130 cm and has steadily increased over that time by about 40 cm. Thus, if we add 2 m of regular spring high tide to the mean height of MIS 5e ($\sim$ +5–6 m) and add storm surges as well (which can easily provide swells of +3 m), we bring a sea crashing onto the rocks within about 5 m of the cave height, and thus there is significant potential for sea spray and moisture in the front of the cave. Given the complete lack of Laminated Facies and LBG Sands in the front of the cave, these sediments were likely eroded out in the front and preserved as a remnant farther in the back.

Following this geogenic disturbance and the deposition of all sediments up to and including LBG Sand, but before DB Sand 3, there was an erosion event of anthropogenic or geogenic origin that was rather localized to the area centered around N98E96. The event is clearly seen in the E96 line section where the LBG Sand is cleanly cut, with some of its top being removed. After MIS 5d, DB Sand 3 drapes cleanly over it and sediment continues to form through MIS 5c. DB Sands 3 and 2 have high frequencies of lithic artifacts and fauna in deposits with significant amounts of burnt organic material, indicating a dense MSA deposit. LB Sand 1 displays lower amounts of organic material, but significant quantities of lithic artifacts and fauna, and then the cave is closed at about 91 ka.

Another cutting event of probable anthropogenic origin can be seen in the N99 line section photograph. One can clearly see that a sloping cut has removed most of the section and was subsequently filled with lighter brown sediment. The cut cleanly sliced through all the sediments of DB Sand 4b through DB Sand 3. This cut was subsequently filled by modern sediments and we now call the fill Northeast Cut Fill. The fill is of late Holocene age, and while the cut is undated, we think it is likely Holocene as well.

The final cutting event is anthropogenic and modern and has already been discussed in Marean et al. (2004). This cutting event occurred sometime in 1999 and the cut material was spilled down the slope of the cave and we collected it. The resulting area has not had time to fill in.

Northeastern area

The Bedrock at the base of the sediments is rounded and represents a high sea level spilling into the cave. Resting on top of this rounded bedrock is the LC-MSA Lower sediments dating to the earlier part of MIS 6. As noted above, there is no remnant of the earlier Laminated Facies, so the contact of the bedrock and LC-MSA Lower likely represents the loss of a significant amount of deposit and time.

The LC-MSA Lower deposit represents a time of significant MSA occupation as represented by the deposition of moderate to high densities of lithic artifacts, shell, mammal bone, and burnt organic material. Following this deposition, there is a minor erosion event or period of lack of sedimentation. The LC-MSA Middle then forms on top of the LC-MSA Lower, near to but perhaps before the transition to MIS 5e. As sea levels were rising with the transition to MIS 5e, significant amounts of sands began to blow into the cave (the older dune in the LC-MSA Upper) and it is likely that there was a dune field on the exposed transgressing coastal platform. Human occupation was present during this period as indicated by significant quantities of lithic artifacts, fauna, shell, and burnt and ashy material.

The LC-MSA Upper indicates a significant sedimentary shift toward lesser anthropogenic input and greater sandy sediment. Lithic artifact and faunal frequencies are less than the sediments below. The lowermost sediments are a hard sandy and silty layer that directly contacts and transitions into the richer archaeological deposits of the LC-MSA Middle. This layer includes multiple lenses of black to dark brown organic material. This is followed by a sandy horizon with a lens of shellfish that probably formed near the MIS 6 and MIS 5e boundary and likely represents dune activity out on the coastal platform. After the MIS 5e high sea stand advanced to its maximum, some of the deposits were eroded away by sea spray and other associated processes.

A second more substantial dune backed up to the cliff and deposited a capping sand layer during MIS 5b that closed the cave to human occupation. A vegetated surface with tree roots formed at the front of the cave on top of the sediments sometime before the cave became nearly closed and after the formation of the dunes. The tree roots penetrated to the top of the LC-MSA Lower and then stopped, except for some very small rootlets. Speleothem then formed in reasonably closed conditions with minor input of sands. Sometime after 39 ka the cave opened and there commenced significant erosion of the sediments, particularly the dunes and their remnants, continuing an erosion front into the now remnant wedge of LC-MSA deposit.

Eastern area

The Eastern area differs from the west in both field and micromorphology observations, and resembles more closely the Northeastern area in overall sedimentary characteristics. The Eastern area has thinner sediments that are deposited more horizontally. There is no evidence for subsidence or faulting of the deposits. There is no preserved Laminated Facies in this area, so it is likely that facies has been entirely eroded away, as it was in the Northeastern area. The sediments have significant quantities of shell. Intact hearths are abundant and they appear as isolated patches more to the south and then bleed together to the north. Unlike the Western area, the sediments have been subjected to pockets of cementation originating from drips from the roof—these drips are clearly visible today.

The bedrock at the base of the sediments is rounded and represents a high sea level reaching into the cave and is almost certainly the same rounded bedrock that we see at the base of the LC-MSA. It is likely that sediments of the LC-MSA Lower formed on this bedrock, but other than a few patches of cemented remnants, these are now eroded away. Following this erosion event, sometime during MIS 5d people occupied this part of the cave (Lower Roof Spall), but only sporadically as indicated by the rather low frequencies of lithic artifacts and fauna; and the major sedimentary input was aeolian sand and roof spall. Transitioning into MIS 5c, human occupation intensified with dense quantities of lithic artifacts and fauna, particularly shellfish, accumulating (Upper Roof Spall and Shelly Brown Sand). The cave was then closed to occupation by a dune, although remnants of this dune have not been found in the Eastern area. After the cave opened after 39 ka there was an erosion event that planed off the top of the sediments, removing greater amounts of deposit to the southern portion of the Eastern area. Onto this truncated surface a thin layer of MSA (Truncation Fill) formed, followed by modern era deposition of eroded MSA from the Western area (Re-Deposited Disturbance).

Acknowledgements

We thank the SAHRA for providing a permit (No. 80/99/04/01/51) to conduct test excavations at the selected sites and HWC for providing subsequent excavation permits. We extend sincere thanks to the Mossel Bay community, and in particular we thank the staff of the Diaz Museum Complex, the Mossel Bay Municipality, Pinnacle Point Developments, and Cape Nature Conservation. We extend a very special thanks to our field and laboratory crew for their outstanding dedication and hard work, as well as specialists for their analyses presented in this report. The financial assistance of the National Research Foundation (NRF): Division for Social Sciences and Humanities (DSSH; South Africa) towards this research is hereby acknowledged (grant # 15/1/3/17/0053 to Nilssen). Opinions expressed in this document and conclusions arrived at, are those of the authors and are not necessarily to be attributed to the NRF: DSSH. The majority of this research was funded by the National Science Foundation (USA; grants # BCS-9912465, BCS-0130713, and BCS-0524087 to Marean), funding from the Huxleys, the Hyde Family Foundation, the Institute for Human Origins, and Arizona State University.

Appendix. Supplementary data

Supplementary data associated with this article can be found in the online version, at doi:10.1016/j.jhevol.2010.07.007.

References

Bernatchez, J.A., 2010. Taphonomic implications of orientation of plotted finds from Pinnacle Point 13B (Mossel Bay, Western Cape Province, South Africa). J. Hum. Evol. 59 (3–4), 274–288.

Birch, G.F.D.P.A., Du Plessis, A., Willis, J.P., 1978. Offshore and onland geological and geophysical investigations in the Wilderness Lakes region. Trans. Geol. Soc. S. Afr. 81, 339–352.

Bird, E.C.F., 2000. Coastal Geomorphology: An Introduction. John Wiley, Chichester.

Brain, C.K., 1981. The Hunters or the Hunted? University of Chicago Press, Chicago.

Brown, K.S., Marean, C.W., Herries, A.I.R., Jacobs, Z., Tribolo, C., Braun, D., Roberts, D.L., Meyer, M.C., Bernatchez, J., 2009. Fire as an engineering tool of early modern humans. Science 325, 859–862.

Clark, J.D., 1959. The Prehistory of Southern Africa. Penguin Books, Baltimore.

Colman, S.M., Pierce, K.L., Birkeland, P.W., 1987. Suggested terminology for Quaternary dating methods. Quatern. Res. 28, 314–319.

Dardis, G.F., Grindley, J.R., 1988. Coastal geomorphology. In: Moon, B.P., Dardis, G.F. (Eds.), The Geomorphology of Southern Africa. Southern Book Publishers, Pretoria, pp. 141–174.

Deacon, H.J., 2001. Modern human emergence: an African archeological perspective. In: Tobias, P.V., Raath, M.A., Maggi-Cecchi, J., Doyle, G.A. (Eds.), Humanity From African Naissance to Coming Millennia - Colloquia in Human Biology and Palaeoanthropology. Florence University Press, Florence, pp. 217–226.

Deacon, H.J., Deacon, J., 1999. Human Beginnings in South Africa. David Philip Publishers, Cape Town.

Deacon, H.J., Geleijnse, V.B., 1988. The stratigraphy and sedimentology of the Main site sequence, Klasies River, South Africa. S. Afr. Archaeol. Bull. 43, 5–14.

Dibble, H., Marean, C., McPherron, S.P., 2007. The use of barcodes in excavation projects: examples from Mossel Bay (South Africa) and Roc de Marsal (France). SAA Archaeol. Rec. January, 33–38.

Dingle, R.V., Rogers, J., 1972. Pleistocene paleogeography of the Agulhus Bank. Trans. Roy. Soc. S. Afr. 40, 155–165.

EPICA Community Members, 2004. Eight glacial cycles from an Antarctic ice core. Nature 429, 623–628.

Erlandson, J.M., 2001. The archaeology of aquatic adaptations: paradigms for a new millennium. J. Archaeol. Res. 9, 287–350.

Fisher, E.C., Bar-Matthews, M., Jerardino, A., Marean, C.W., 2010. Middle and late Pleistocene paleoscape modeling along the southern coast of South Africa. Quatern. Sci. Rev. 29, 1382–1398.

Flemming, B.W., 1983. Sediment dynamics on the inner Agulhus Bank. S. Afr. J. Sci. 79, 160.

Flemming, B.W., Martin, A.K., Rogers, J., 1983. Onshore and Offshore Coastal Aeolianites between Mossel Bay and Knysna, University of Cape Town Marine Geoscience Unit 14, pp. 151–160.

Goldberg, P., Sherwood, S., 2006. Deciphering human prehistory through the geoarcheological study of cave sediments. Evol. Anthropol. 15, 20–36.

Herries, A.I.R., Fisher, E.C., 2010. Multidimensional modeling of magnetic mineralogy as a proxy for fire use and spatial patterning: evidence from the Middle Stone Age bearing sea cave of Pinnacle Point 13B (Western Cape, South Africa). J. Hum. Evol. 59 (3–4), 306–320.

Henshilwood, C.S., D'Errico, F., Yates, R., Jacobs, Z., Tribolo, C., Duller, G.A.T., Mercier, N., Sealy, J.C., Valladas, H., Watts, I., Wintle, A.G., 2002. Emergence of modern human behavior: Middle Stone Age engravings from South Africa. Science 295, 1278–1280.

Henshilwood, C.S., D'Errico, F., Vanhaeren, M., van Niekerk, K., Jacobs, Z., 2004. Middle Stone Age shell beads from South Africa. Science 304, 404.

Illenberger, W.K., 1996. The geomorphologic evolution of the wilderness dune cordons, South Africa. Quatern. Intl. 33, 11–20.

Jacobs, Z., 2010. An OSL chronology for the sedimentary deposits from Pinnacle Point Cave 13B - a punctuated presence. J. Hum. Evol. 59 (3–4), 289–305.

Jacobs, Z., Duller, G.A.T., Wintle, A.G., Henshilwood, C.S., 2006. Extending the chronology of deposits at Blombos Cave, South Africa, back to 140 ka using optical dating of single and multiple grains of quartz. J. Hum. Evol. 51, 255–273.

Jacobs, Z., Roberts, R.G., Galbraith, R.F., Deacon, H.J., Grun, R., Mackay, A., Mitchell, P., Vogelsang, R., Wadley, L., 2008. Ages for the Middle Stone Age of southern Africa: implications for human behavior and dispersal. Science 322, 733–735.

Karkanas, P., Bar-Yosef, O., Goldberg, P., Weiner, S., 2000. Diagenesis in prehistoric caves: the use of minerals that form in situ to assess the completeness of the archaeological record. J. Archaeol. Sci. 27, 915–930.

Karkanas, P., Goldberg, P., 2010. Site formation processes in Site PP13B (Pinnacle Point, South Africa): resolving stratigraphic and depositional complexities with micromorphology. J. Hum. Evol. 59 (3–4), 256–273.

Laville, H., Rigaud, J.P., Sackett, J., 1980. Rock Shelters of the Perigord: Geological Stratigraphy and Archaeological Succession. Academic Press, New York.

Malan, J.A., 1987. The Bredasdorp group in the area between Gans Bay and Mossel Bay. S. Afr. J. Sci. 83, 506–507.

Malan, J.A., 1991. Lithostratigraphy of the Klein Brak Formation (Bredarsdorp Group). In: South African Committee for Stratigraphy: Lithostratigraphic Series, vol. 13. Department of Mineral and Energy Affairs, Geological Survey. 1–13.

Marean, C.W., 2010. Pinnacle Point Cave 13B (Western Cape Province, South Africa) in context: the Cape floral kingdom, shellfish, and modern human origins. J. Hum. Evol. 59 (3–4), 425–443.

Marean, C.W., Assefa, Z., 2005. The Middle and Upper Pleistocene African record for the biological and behavioral origins of modern humans. In: Stahl, A.B. (Ed.), African Archaeology. Blackwell, New York, pp. 93–129.

Marean, C.W., Bar-Matthews, M., Bernatchez, J., Fisher, E., Goldberg, P., Herries, A.I.R., Jacobs, Z., Jerardino, A., Karkanas, P., Minichillo, T., Nilssen, P.J., Thompson, E., Watts, I., Williams, H.M., 2007. Early human use of marine resources and pigment in South Africa during the Middle Pleistocene. Nature 449, 905–908.

Marean, C.W., Nilssen, P.J., Brown, K., Jerardino, A., Stynder, D., 2004. Paleoanthropological investigations of Middle Stone Age sites at Pinnacle Point, Mossel Bay (South Africa): archaeology and hominid remains from the 2000 field season. J. Paleoanthroopl. 2, 14–83.

McDermott, F., 2004. Palaeo-climate reconstruction from stable isotope variations in speleothems: a review. Quatern. Sci. Rev. 23, 901–918.

Murray, A.S., Wintle, A.G., 2000. Luminescence dating of quartz using an improved single-aliquot regenerative-dose protocol. Rad. Meas. 32, 57–73.

Partridge, T.C., 1997. Cainozoic environmental change in southern Africa, with special emphasis on the last 200 000 years. Prog. Phys. Geogr. 21, 3–22.

Partridge, T.C., Maud, R.R., 1987. Geomorphic evolution of southern Africa since the Mesozoic. S. Afr. J. Geol. 90, 179–208.

Reading, H.G., 1996. Sedimentary Environments: Processes, Facies and Stratigraphy. Blackwell, Boston.

Sampson, C.G., 1971. The Stone Age Archaeology of Southern Africa. Academic Press, New York.

Singer, R., Wymer, J., 1982. The Middle Stone Age at Klasies River Mouth. The University of Chicago Press, Chicago.

Tinley, K.L., 1985. Coastal dunes of South Africa. In: South African National Scientific Programmes, vol. 109. Foundation for Research Development, Council for Scientific and Industrial Research, Pretoria, South Africa, pp. 1–300.

Van Andel, T.H., 1989. Late Pleistocene sea levels and human exploitation of the shore and shelf of southern South Africa. J. Field Archaeol. 16, 133–155.

Viljoen, J.H.A., Malan, J.A., 1993. Die Geologie van die Gebiede 3421 BB Mosselbaai en 3422 AA Herbertsdale. Department of Mineral and Energy Affairs, Pretoria.

Weiner, S., Goldberg, P., Bar-Yosef, O., 1993. Bone preservation in Kebara Cave, Israel using on-site Fourier transform infrared spectrometry. J. Archaeol. Sci. 20, 613–627.

Wolf, P.R., Ghilani, C.D., 2002. Elementary Surveying: An Introduction to Geomatics. Prentice-Hall, Upper Saddle River, N.J.

Woodward, J.C., Goldberg, P., 2001. The sedimentary records in Mediterranean rockshelters and caves: archives of environmental change. Geoarchaeol. Intl. J. 16, 327–354.